

OPTIMUM DESIGN OF LAMINATED COMPOSITE STRUCTURES  
FOR ENHANCED DAMPING CHARACTERISTICS

BY

CHIEN-JONG SHIH

A DISSERTATION PRESENTED TO THE GRADUATE SCHOOL  
OF THE UNIVERSITY OF FLORIDA IN PARTIAL FULFILLMENT  
OF THE REQUIREMENTS FOR THE DEGREE OF DOCTOR OF PHILOSOPHY

UNIVERSITY OF FLORIDA

1989

To the Glory of God

#### ACKNOWLEDGEMENTS

I would like to express my deepest thanks to Dr. Prabhat Hajela, the chairman of supervisory committee, for his friendship, constructive guidance and the freedom to experiment, discover, fail and succeed.

I am grateful to committee member Dr. C.T. Sun for his encouragement and his constant willingness to discuss the subject matter. I also express my thanks to Dr. L.E. Malvern, Dr. G. Piotrowski and Dr. B.V. Sankar for serving on the supervisory committee and for their constant support.

Finally, I would like to acknowledge the Army Research Office for support of this work under Grant DAAL03-88-K0013.

## TABLE OF CONTENTS

	<u>page</u>
ACKNOWLEDGEMENTS . . . . .	iii
ABSTRACT . . . . .	vi
CHAPTERS	
I INTRODUCTION . . . . .	1
I.1 Literature Survey . . . . .	4
I.2 Scope of Present Research . . . . .	10
II NONLINEAR OPTIMIZATION WITH MIXED INTEGER AND DISCRETE DESIGN VARIABLES . . . . .	12
II.1 Introduction . . . . .	12
II.2 Theoretical Background and Problem Formulation . . . . .	14
II.3 Modified Branch-and-Bound Search . . . . .	22
II.4 Illustrative Example . . . . .	26
III MULTIOBJECTIVE OPTIMIZATION WITH MIXED INTEGER AND DISCRETE DESIGN VARIABLES . . . . .	53
III.1 Introduction . . . . .	53
III.2 Multiobjective Optimum Design with Mixed Variables . . . . .	55
III.3 Illustrative Example . . . . .	62
IV OPTIMUM SYNTHESIS OF SHORT FIBER COMPOSITES FOR IMPROVED INTERNAL MATERIAL DAMPING . . . . .	75
IV.1 Introduction . . . . .	75
IV.2 Analytical Estimates of Damping by Cox's Shear-Lag model . . . . .	77
IV.3 Formulation of an Advanced Shear-Lag Model to Obtain Internal Damping . . . . .	83
IV.4 Optimum Synthesis Problem . . . . .	99

V	MULTIOBJECTIVE OPTIMIZATION FOR IMPROVED STRUCTURAL DAMPING AND VIBRATION CONTROL . . . .	113
V.1	Introduction . . . . .	113
V.2	Analytical Estimates of Structural Damping and Displacement for a Cantilever Beam . .	115
V.3	Formulation of Multiobjective Optimum Design with Mixed Design Variables . . . .	122
V.4	Multiobjective Optimum Design for Dynamically Responding Composite Structure.	125
VI	CONCLUDING REMARKS . . . . .	137
VI.1	Conclusions . . . . .	138
VI.1	Recommendations for Future Work . . . . .	141
	REFERENCES . . . . .	143
	BIOGRAPHICAL SKETCH . . . . .	150

Abstract of Dissertation Presented to the Graduate School  
of the University of Florida in Partial Fulfillment of the  
Requirements for the Degree of Doctor of Philosophy

OPTIMUM DESIGN OF LAMINATED COMPOSITE STRUCTURES  
FOR ENHANCED DAMPING CHARACTERISTICS

By

Chien-Jong Shih

May, 1989

Chairman: Prabhat Hajela

Major Department: Aerospace Engineering, Mechanics and  
Engineering Science

A multicriterion optimization algorithm involving a mix of discrete, integer and real continuous design variables is developed. This algorithm involves a min-max variant of the modified global criterion approach in conjunction with a modified branch and bound method. The use of a weighting strategy with this proposed algorithm allows the generation of a set of Pareto optimal (noninferior) solutions for both convex and nonconvex problems.

There are two special features in this development. First, the proposed modification of the branch-and-bound approach is based on a piecewise linear approximation to solve the nonlinear single objective function optimization problem with mixed design variables. Second, the proposed modified global criterion method is based on an equivalent

scalar optimization. Also, the global criterion approach is critically dependent on obtaining an ideal solution, which, for mixed design variables is shown to be a solution of the continuous optimization problem.

The methodology developed in this research is applied to a class of engineering design problems. The specific area of interest is the design of laminated composite structures for enhanced structural damping. Such designs must also conform to requirements of minimum structural weight and dynamic displacements in a dynamic loading environment. The structural damping characteristics can be improved by both internal material damping and by the addition of viscoelastic layers to the base structure.

## CHAPTER I

### INTRODUCTION

Recent years have witnessed an increased application of laminated composite materials in structures that are subjected to dynamic loads. In some cases, the loading introduces near resonant conditions, and an enhanced level of internal damping in the structural system provides the most direct passive approach for controlling undesirable vibrations [1]. Active vibration control has also been studied extensively and its methodology and application are the subject of several recent publications [2,3]. The present research problem is, however, restricted to damping enhancements via passive methods. Materials with a high level of internal damping also typically possess low structural stiffness, and this introduces a need to carefully tailor the structure for the desired stiffness and damping characteristics. In addition to this, the weight requirements of structural components for applications in aircraft, spacecraft and automotive vehicles have also become increasingly stringent, with a preference for lighter, stiffer structures. The achievement of these goals presents challenging problems from the standpoint of design and synthesis. The use of formal optimization methods in



conjunction with refined analysis techniques provides a useful approach to this problem.

The origins of contemporary developments in structural optimization can be traced to a publication of Schmit [4]. This paper was the first to demonstrate the potential of using nonlinear programming methods to obtain the optimum design of structural systems. Since this publication, there have been numerous attempts at exploring the optimum structural sizing problem, with varying degrees of complexity. References [5-8] are typical of such efforts. New advancements in digital computing technology have further contributed to a maturing of this discipline, with the introduction of efficient methods applicable to more realistic design problems.

A typical structural optimization problem may involve the selection of optimal cross sections of structural members to obtain a minimum weight configuration with respect to some failure criteria. This can be alternatively described in optimization terminology as the selection of optimum design variables which meet the functional requirements of minimizing or maximizing an objective function, and simultaneously satisfying a set of design constraints. The digital computer is ideally suited for an implementation of optimization algorithms, as the design space is systematically explored in preferred search directions. A significant amount of research effort has

been expended in developing applicable search algorithms, with notable contributions from the mathematics and operations research community. A large number of such constrained search strategies are applicable to design spaces in which the design variables are assumed to vary continuously.

In several practical applications of interest, such as in composite structures, design variables may vary discretely or as integers. The ability to account for such integer and discrete variations calls for the use of integer programming and discrete programming methods in optimization. This problem belongs to the category of mixed programming problems which involve a mix of discrete, integer and real continuous variables, and requires the development of a search strategy that suitably accounts for these complexities. A traditional gradient based approach is not always applicable because of the discontinuous nature of the design space.

An additional degree of difficulty may be introduced in optimization problems where the scalar objective is replaced by two or more distinct objective functions. Such problems belong to the class of multicriterion optimization problems and are encountered in problems of practical interest. The criteria are often conflicting in that an improvement in one measure is generally at the expense of another. Such multiobjective optimization problems have been studied in

literature, and in the present study they are examined in conjunction with discrete and integer design variables.

The following section of this chapter presents a historical perspective relating to the development of optimization methodology. A brief survey of developments in analytical and experimental determination of damping in composite structural elements is also presented.

### I.1 Literature Survey

Optimization methods have found numerous applications in broad areas of engineering, economics and operations research [9]. Since the early 1960s, there have been a significant number of reports describing the development of new algorithms, the implementation of which was made possible by rapid advances in digital computing capabilities. The most general solution strategies for optimization problems are a class of mathematical programming algorithms, which themselves can be further categorized as linear programming (LP) and nonlinear programming (NLP) approaches. Linear programming techniques are widely used to solve a number of military, economic, industrial and societal problems. In a 1976 survey of American companies [10], LP came out as the most widely used method (74%) among all the optimization methods. This can largely be attributed to widely available commercial software. References [11] and [12] provide a useful source

for understanding both the theoretical aspects of linear programming and its applications in problems of practical interest. Nonlinear programming strategies are of interest in problems where either the objective or at least one of the constraint function is nonlinear. References [13] and [14] provide perspectives of both theoretical analysis and engineering applications.

For practical applications encountered in operations research and econometrics, problems of linear programming with integer or discrete solutions are of significant importance. Accordingly, these requirements gave rise to integer programming and discrete programming methods. Surveys on methods for solving linear integer programming problems can be found in [15,16]. In practice, one encounters problems involving a mix of integer, discrete and continuous variables. A number of integer linear programming or mixed linear programming commercial codes are now available. A majority of such codes are based on the branch and bound method [17,18,19,20]. The theoretical basis of this method and its scope is presented in [21].

In many applications of practical importance, the design space in nonlinear programming problems could also consist of continuous, discrete, or even integer solutions. Such problems may be formulated as nonlinear mixed integer programming or discrete optimization problems. The solution strategy for a nonlinear, mixed integer programming problem

was first proposed by Garfinkel and Nemhauser [22]. Other researches [23] have examined an extension of this work by considering a nonlinear programming problem with integer and discrete variables. A survey conducted in the present work failed to produce any prior work involving a mix of discrete, integer and continuous variables in nonlinear problems.

Over the past two decades, there has been an increased awareness of the need to identify and consider simultaneously several objective criteria in an optimization problem. This has led to the emergence of the well-recognized Multicriteria Programming (MCP), also referred to as the multiobjective optimization or vector optimization problem. In such problems, the components of the vector objective criterion may be in conflict with each other. Hence, 'optimization' means finding a solution which would yield acceptable values for all the objective criteria. One of the earliest efforts in this area may be attributed to an Italian economist, Pareto, who in 1896 introduced the concept within the framework of welfare economics [24]. The ramifications of this work in optimization theory, operations research, and control theory were recognized only in the late 1960s. There have been fewer applications than theoretical developments, but the successful uses of MCP keep growing. There is a large array of analytical techniques available for the multicriterion problems. Cohon

[25] and Hwang and Masud [26] present comprehensive surveys of this area. Another survey due to Zeleny [27] provides an excellent treatment of the entire multicriterion endeavour. Goicoechea, Hensen and Duckstein [28] offer broad coverage of the field with many examples from engineering, particularly water-resources engineering. An application of multicriterion optimization in structural design is presented in [29]. Theoretical considerations may also be found in [30], which focuses on existence, necessary/sufficient conditions, stability, Lagrange duality, and conjugate duality for efficient solutions in such problems. However, the full potential of multicriterion optimization is not yet realized. In particular, the application of such methods in problems with mixed integer, discrete, and continuous design variables must be examined in more extensive detail. This constitutes a major contribution of the present work.

Although the domain of applicability of such methods is extensive, the present work is restricted to examining design problems pertaining to composite structural components. This area has received increased attention in recent years, and several publications attest to this general interest. Tauchert and Adibhatla [31] investigate a problem where the objective criterion is defined in terms of minimum strain energy and maximum failure load in composite elastic beams. Bauchau [32] maximizes the first natural

bending frequency of the rotating graphite/epoxy shaft through an adequate tapering of the wall thickness. Liao, Sung, and Thompson [33] formulate a problem with the objective of maximizing the damping capacity in a composite specimen. The design variables in this problem are fiber orientation and ply thickness. The subject of damping in composites and design for maximum damping is extensively explained in the present work.

In 1927, Kimball and Lovell [34] performed an experiment that allowed them to conclude that damping (internal friction loss) is a material property. Numerical values for the material damping were shown to range from 0.00001 to 0.2 [34,35]. Due to an increased application of composites in structures, the damping characteristics of composites have received greater attention. In another experimental study, Suarez et al. [36] observed the dependence of damping on frequency in fiber reinforced epoxy components. High values of material damping of short fiber composites were analytically predicted and experimentally demonstrated in references [37] and [38]. Sun and his co-workers have developed theoretical relationships for the material damping of short fiber-reinforced polymer matrix composites under off-axis loading [39,40]. They developed relationships for the loss and storage moduli in terms of the fiber aspect ratio, loading angle, stiffness of the fiber and matrix materials, the fiber volume fraction, and

the damping properties of the fiber and matrix materials. They also conducted parametric studies to examine the variation of the damping with the fiber aspect ratio and the loading angle in order to determine optimum values of these parameters for maximum internal damping. However, parametric studies of this form have been shown to yield suboptimal results. The present work proposes a design synthesis approach based on formal multivariable optimization to maximize the internal material damping. Two distinct analysis models, Cox's shear-lag theory and an advanced shear-lag model, are used in the present research.

One of the earliest attempts to enhance damping characteristics of basic composite structures can be attributed to Plunkett and Lee [41]. They examined the changes in damping properties of a beam due to the application of constrained viscoelastic layers on the top and bottom of the structure. Recently, the addition of viscoelastic material for increasing the structural damping in metallic structural elements has been proposed by Nashif et al. [42]. Sun et al. have recently presented [43] the results of a study wherein the damping in polymer matrix composite structures is increased by application of viscoelastic layers. Both analytical predictions and experimental verifications are presented. Their results are valuable from the standpoint of providing a greater understanding of the potential of the approach but are not



as readily adaptable for design synthesis.

The present research proposes a multiobjective optimization procedure in conjunction with a mix of design variables in order to maximize the structural damping, including internal material damping. This proposition also includes a consideration of minimizing the structural weight and vibrational displacement at the same time.

### I.2 Scope of Present Research

The scope of the present work and its organization can be summarized as follows.

The second chapter introduces a general formulation of the nonlinear optimization problem. It also provides a brief overview of an NLP-based algorithm used in the present work. Details of a nonlinear, mixed programming code NMIDOPT, capable of handling a nonlinear optimization problem involving a mix of integer, discrete, and continuous design variables are presented. The application of this algorithm to a class of representative structural design problems is also presented and discussed.

Chapter three describes the development of a nonlinear, multicriterion optimization algorithm. This algorithm can deal with several noncommensurable objectives simultaneously and can accommodate a mix of integer, discrete, and continuous design variables. The applicability of the proposed algorithm is demonstrated by the design of

statically loaded isotropic and laminated cantilever beams. The results are presented and discussed.

In chapter four, the analysis and design of structural composites for maximum internal damping is posed as a multivariable optimization problem. Two distinct analytical models to predict internal damping in short fiber composites are proposed. These models are based on Cox's shear-lag analysis and on a modification termed here as an advanced shear-lag theory. The latter allows for the matrix material to sustain axial loads and is applicable in cases where the extensional modulus of the matrix material is not negligible in comparison to the fiber material. The multivariable optimization formulation is used to maximize the internal damping characteristic of representative composite elements.

Chapter five extends the internal damping enhancement problem by including contributions to damping from external viscoelastic tapes that are bonded to the structure. The optimum design problem is one in which the structural damping is maximized and the weight and dynamic displacements are minimized, using the multiobjective optimization algorithm for the mixed design variable space.

Conclusions drawn from this study and recommendations for future research are presented in the final chapter.

## CHAPTER II

### NONLINEAR OPTIMIZATION WITH MIXED INTEGER AND DISCRETE DESIGN VARIABLES

#### II.1 Introduction

Nonlinear programming based optimization algorithms provide a viable tool for applications in optimum structural design. These methods are primarily applicable in problems where the design space is defined in terms of continuous design variables. In several applications of practical significance, however, the design space could consist of continuous, discrete, or even integer design variables. Such problems have been frequently approached by considering all design variables as continuous, obtaining the optimum solution, and then rounding the specific variables either up or down, to the nearest integer or discrete point. This simple rounding procedure often fails completely, resulting in either a suboptimal design or, in some cases, an infeasible design [44].

Early efforts in obtaining a systematic solution to the integer linear programming problem are available in the work of Gomory [45]. These methods resulted in obtaining dual feasible solutions, which required an optimal integer solution as a condition for a primal feasible integer

solution. The branch-and-bound algorithms that emerged later were based on enumeration of the space of all feasible integer solutions. The algorithm due to Land and Doig [46] was one of the earliest efforts in this direction. This algorithm had a very significant demand on the storage, a limitation that was later overcome in Dakin's version of the algorithm [47]. The use of the term branch-and-bound first appeared in a publication by Little et al. [48], where the algorithm was used to obtain a solution to the traveling salesman problem. A detailed explanation of the branch-and-bound approach is also available in [49].

The general framework for solving an integer programming problem involves decomposing the original problem into subproblems, modifying constraints to enlarge feasible domains, and finally a process referred to as fathoming. Fathoming involves checking a solution for feasibility and establishing its optimality.

The basic solution strategy used in this work for nonlinear mixed integer programming problems is a variant of the approach proposed by Garfinkel and Nemhauser [22]. The strategy consists of a systematic search of continuous solutions in which the discrete and integer variables are successively forced to assume specific values. The logical structure of the set of solutions was constructed as a binary tree. A modified feasible directions algorithm [50] was used in the solution of the continuous nonlinear

programming problem, with piecewise linear representation of the objective function and constraints. Details of this approach are presented in subsequent sections of the paper. The application of this algorithm is then explored in practical structural design, which mandates a need to take into consideration continuous, discrete, and integer design variables. Specific examples include an optimal design of a structural welded beam for minimum cost and constraints on stress and buckling, and a composite laminate beam sized for minimum weight and constraints on strength, displacement, and natural frequencies.

## II.2 Theoretical Background and Problem Formulation

Numerical optimization methods have gone through an extensive process of development over the past two and a half decades. The purpose of numerical optimization can best be defined as an aid to the designer to rationally search for the best design to meet prescribed requirements. However, it is important to recognize that the use of numerical optimization techniques will seldom, if ever, yield the absolute best design. Hence, a better definition of these techniques may be had by replacing the word "optimization," with "design improvement."

In an engineering optimization problem, the numerical quantities for which values are to be chosen will be called design variables or decision variables. In each engineering

task there are some restrictions dictated by the environment, processes, and/or resources, which must be satisfied in order to produce an acceptable solution. These requirements are called constraint functions and describe dependencies among design variables and other parameters. These dependencies are written in the form of mathematical inequalities or equalities. In the process of selecting a "best solution" from all solutions which satisfy the constraints, there must exist a criterion which allows these solutions to be compared. This criterion is an integral part of the problem formulation, and in the optimization model, must be expressed as a computable function of the decision variables. This function is called the objective function.

The general nonlinear constrained optimization problem can mathematically be formulated as follows:

$$\text{Minimize:} \quad F(X) \quad \text{Objective function} \quad (2.1)$$

Subject to:

$$g_j(X) \leq 0 \quad j=1,m \quad \text{inequality constraints} \quad (2.2)$$

$$h_k(X) = 0 \quad k=1,\ell \quad \text{equality constraints} \quad (2.3)$$

$$x_i^l \leq x_i \leq x_i^u \quad i=1,n \quad \text{side constraints} \quad (2.4)$$

where  $X = [x_1, x_2, \dots, x_n]^T$  is a vector of design variables. The  $x_i^l$  and  $x_i^u$  represent the lower and upper bounds on the design variables, respectively.

If equality constraints are explicit in  $X$ , they can often be used to reduce the number of design variables. Although side constraints (Eqn. (2.4)) could be included in the inequality constraint set given by Eqn. (2.2), it is usually convenient to treat them separately as they define the region of search for the optimum. If a particular optimization problem requires maximization, we simply minimize  $-F(X)$ .

Most optimization algorithms require that an initial set of design variables  $X^0$  be specified. From this starting point, the design is updated iteratively, with the most generally used iterative update equation as follows

$$\{X^q\} = \{X^{q-1}\} + \alpha^* \{S^q\} \quad (2.5)$$

where  $q$  is the iteration number and  $S$  is a vector search direction in the design space. The scalar quantity  $\alpha^*$  defines the step in the search direction  $S$  at the  $q$ -th iteration. Each search direction has to reduce or maintain constant the objective function without violating the design constraints. This can be better described by referring to

the method of feasible-usable search directions [51].

Figure 2.1 shows lines of constant objective function and constraints, plotted for two design variables. At a point  $\{X^0\}$ , the tangents to the contours of constant objective function value,  $F(X)$ , and the constraint,  $g_1(X)$ , are defined. These tangents bound the space of possible usable-feasible search directions. A direction that forms an obtuse angle with the normal to the tangent of object function, will either reduce or hold constant the value of objective function. The space of such search directions defines the usable sector. Similarly, a hyperplane tangent to the constraint surface at point  $\{X^0\}$  will bound the feasible sector, which is defined as the region in which the design constraint is not violated. The search direction must fall in the usable-feasible region where the constraint is satisfied and the objective function decreases or remains constant.

From a practical standpoint, the best approach is usually to start the optimization process from several different initial vectors, and if the optimization results in essentially the same final design, we can be reasonably assured that this is the true optimum. However, it is possible to check optimality on the basis of derivable conditions. Furthermore, we can also show that under certain circumstances, these necessary conditions are also sufficient to ensure that the solution is a global optimum.



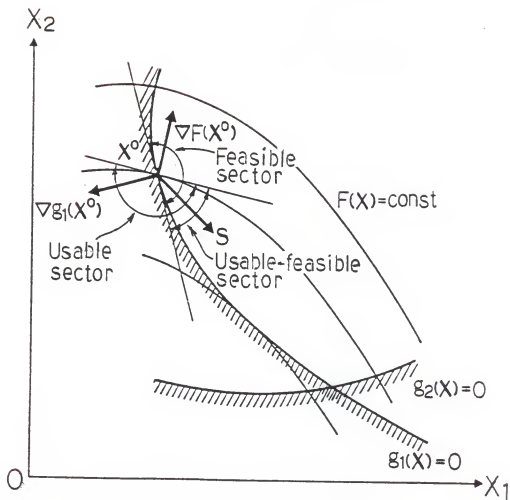


Figure 2.1 Method of feasible usable search direction.

For the optimization problem design in Eqns. (2.1) to (2.4), the necessary conditions for optimality are referred to as Kuhn-Tucker conditions [51], and are defined as follows.

$$1. \quad X^* \text{ is feasible.} \quad (2.6)$$

$$2. \quad \lambda_j g_j(X^*) = 0 \quad j=1, m \quad \lambda_j \geq 0 \quad (2.7)$$

$$3. \quad \nabla F(X^*) + \sum_{j=1}^m \lambda_j \nabla g_j(X^*) + \sum_{k=1}^l \lambda_{k+m} \nabla h_k(X^*) = 0 \quad (2.8)$$

$$\lambda_j \geq 0 \quad (2.9)$$

$$\lambda_{m+k} \quad \text{unrestricted in sign} \quad (2.10)$$

Here  $X^*$  defines the optimum design and  $\lambda_j$  are the Lagrange multipliers. If the objective function and all constraint functions are convex, the design space is said to be convex, and the necessary Kuhn-Tucker conditions are also sufficient to guarantee that the optimum is a global optimum. A detailed discussion of the sufficiency requirements can be found in [52].

To improve computational efficiency in nonlinear optimization problems, a piecewise linearization of the design space is frequently adopted. Consider the general nonlinear programming problem of Eqns. (2.1) to (2.4). This problem may be linearized via a first-order Taylor series

expansion to obtain the following.

$$\text{Minimize: } F(X) \approx F(X^0) + \nabla F(X^0) \delta X \quad (2.11)$$

Subject to

$$g_j(X) \approx g_j(X^0) + \nabla g_j(X^0) \delta X \leq 0 \quad j=1, m \quad (2.12)$$

$$h_k(X) \approx h_k(X^0) + \nabla h_k(X^0) \delta X = 0 \quad k=1, \ell \quad (2.13)$$

$$X_i^l \leq X_i + \delta X_i \leq X_i^u \quad i=1, n \quad (2.14)$$

$$\text{where } \delta X = X - X^0 \quad (2.15)$$

The zero superscript identifies the point about which this Taylor series expansion is performed.

For nonlinear problems, it is essential that appropriate move limits be established [53]. By allowing the design variables to change only within some percentage of their initial point values, the inaccuracies introduced due to the linear approximations are reduced. An example of limiting the movement of the design variables in this manner can be seen in Figure 2.2. A larger move limit, as seen in case B, results in a greater error due to the linear approximation than that in case A. In practice, these move

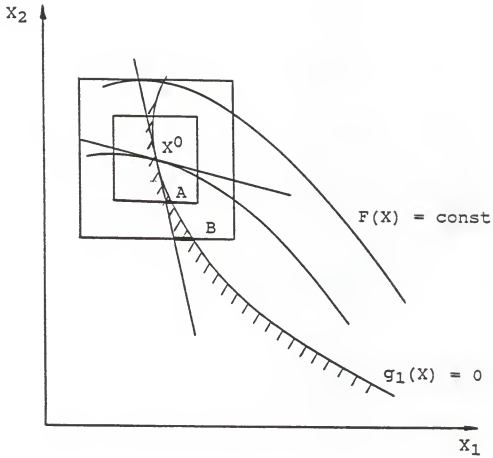


Figure 2.2 Effect of move limit choice on constraint violation.

limits are reduced during the optimization process, so that a solution is found to the desired accuracy. This piecewise linearization process was used in the branch-and-bound strategy for handling discrete/integer variables. The branch-and-bound search is described in the following section.

### II.3 Modified Branch-and-Bound Search

The mathematical formulation of an optimization problem with mixed continuous, discrete, and integer variables can be stated as follows.

$$\text{Minimize} \quad F(\bar{x}) \quad (2.16)$$

$$\text{Subject to} \quad g_j(\bar{x}) \leq 0 \quad j=1,2,\dots,p \quad (2.17)$$

$$h_k(\bar{x}) = 0 \quad k=1,2,\dots,s \quad (2.18)$$

$$x_i^l \leq x_i \leq x_i^u \quad (2.19)$$

$$\{\bar{x}\} = \{x_1, x_2, \dots, x_L, \dots, x_m, \dots, x_n\} \quad (2.20)$$

where the  $n$ -vector of design variables  $\{\bar{x}\}$  contains  $L$  nonnegative discrete variables,  $m-L$  nonnegative integer variables, and  $n-m$  positive real variables. The case of  $L=0$  represents the nonlinear integer programming problem. The objective function  $F(\bar{x})$  and constraints  $g_j(\bar{x}) \leq 0$  and  $h_k(\bar{x}) = 0$  are typically nonlinear but may be represented by a linear approximation for a limited range of design

variable changes. Such lower and upper bounds on the design variables are indicated by  $x_i^l$  and  $x_i^u$ , respectively. Despite the fact that both the objective function and constraints are represented by linear approximations, the discrete and integer design variables render the problem nonlinear.

A solution to the above mixed integer discrete programming problem proceeds as follows. As a first step, the requirements that appropriate variables be discrete or integer are relaxed, and a solution of the continuous problem is obtained. If the solution is such that the original requirements on integrality and discreteness are satisfied, and the design is feasible, an optimal design is obtained. This is not a likely scenario and one or more variables that are obtained from the continuous solution may violate the original requirements. A branch node may be introduced at any one of these nodes. As an example of how branching occurs, one may consider a variable  $x_i$  that assumes values from an ordered discrete set  $\{d_1, d_2, \dots, d_p\}$ . The bounds on the continuous problem were so chosen that there must exist an index  $j$  that is between 1 and  $p$ , for which the following is satisfied.

$$d_j < x_i < d_{j+1} \quad (2.21)$$

Two new subproblems are generated, one with a new lower

bound  $x_i \geq d_{j+1}$  and another with a new upper bound  $x_i \leq d_j$ . This process of forming new subproblems is called branching. In a similar manner, if  $x_j$  is obtained as a solution to the continuous problem, and it is actually required to be an integer value, then  $x_j$  is expressed as a sum of integer and fractional values as follows,

$$x_j = I_j + r_j \quad (2.22)$$

where  $I_j$  is an integral value and  $0 < r_j < 1$ . As for the case with discrete variables, a branch is created with the generation of two new subproblems, the first with an upper bound of  $x_j \leq I_j$  and another with a lower bound constraint  $x_j \geq I_j + 1$ . The branching actually eliminates that portion of the feasible continuous space that does not admit feasible integer or discrete solutions. The subproblems created above are again solved as continuous problems and the optimal solutions to these problems are stored at the node locations. This branch and bound procedure is successively applied until a feasible integer and discrete design set is obtained, and the corresponding value of the objective function is taken as the upper bound for the optimization problem. At this juncture, all nodes of the continuous solution with an objective function higher than the upper bound can be eliminated from further consideration, and these nodes are considered fathomed. Additional conditions

under which a node is considered fathomed are as follows.

- a) The continuous variable solution is also a feasible, discrete/integer solution.
- b) The continuous solution is infeasible.
- c) The optimal objective function obtained for the continuous problem is higher than the present upper bound.

This procedure of branch and bound is carried out for all unfathomed nodes. Whenever a new discrete or integer feasible solution is obtained, and the objective function corresponding to this solution is lower than the current upper bound, the new objective function replaces the upper bound. When all the possible nodes have been fathomed, the most superior discrete-integer solution is taken as the optimal solution to the original problem. The methodology is best illustrated by a flowchart of the computer implementation and by numerical examples presented in subsequent sections. It is worthwhile to note that the maximum number of nodes at which information is stored is given as  $(2^{(N+1)}-1)$ , where  $N$  is equal to the total number of integer or discrete type variables.

A computer code NMIDOPT was generated for the implementation of the proposed branch and bound approach. The organization of the code is modular, and there are three



major subroutines that are employed for distinct operations. Subroutine ITP was used to execute the branch and bound procedure and to create the subproblems. The nonlinear, continuous optimization problem of each branch was solved in NOP, which uses a modified feasible directions algorithm [50]. In the present approach, an option existed of solving either the exact nonlinear optimization problem or a piecewise linear approximation of this problem with adequate lower and upper bounds imposed on the design variable change. A third subroutine, JUDGE, was used to determine whether a node was fathomed and to update the current upper bound of the problem. A brief flow chart for the procedure is shown in Figure 2.3. A detailed flow chart of NMIDOPT and all associated subroutines is shown in Figure 2.4 to 2.6.

#### II.4 Illustrative Example

To illustrate the branch and bound process, the algorithm was used in the minimum cost design of a welded beam structure shown in Figure 2.7, with constraints on weld stresses, buckling loads, bar deflections, and bending stresses. This example, borrowed from [54], has been used in a study related to integer programming algorithms [23]. Detailed expressions for the objective function and constraints for the problem can be had from these publications. For our purposes, it suffices to state that

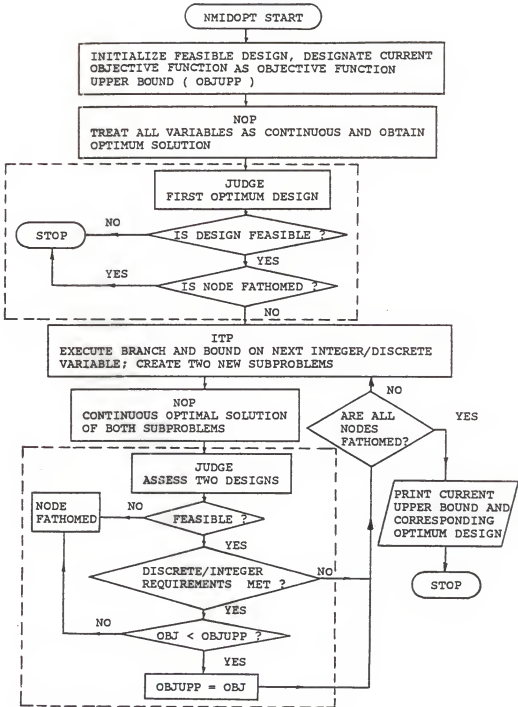


Figure 2.3 Flow diagram representation of code NMIDOPT for mixed integer and discrete programming in nonlinear optimization.

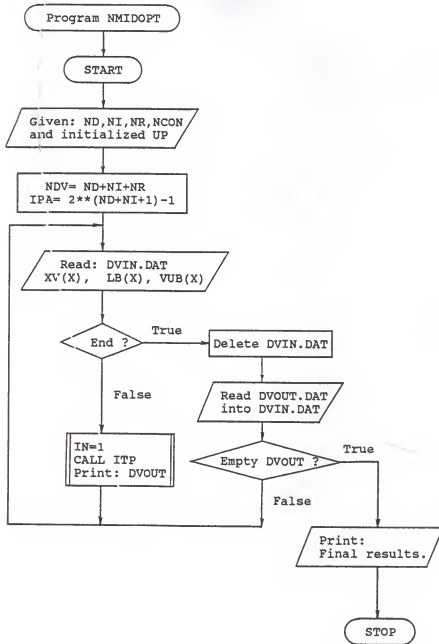


Figure 2.4 Flowchart for the controlling algorithm of NMIDOPT.

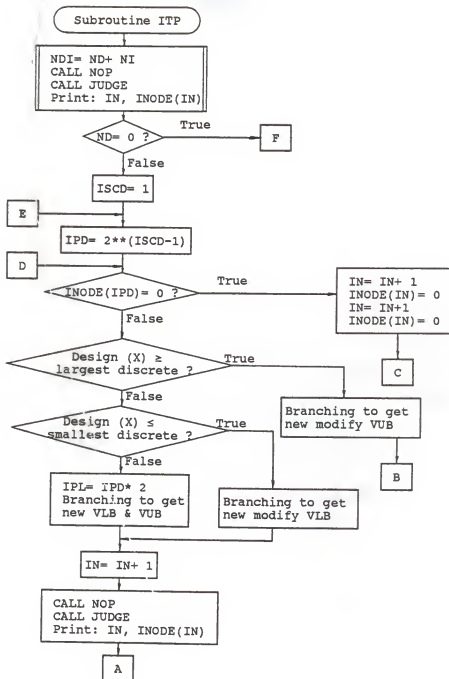


Figure 2.5 Flowchart for the subroutine ITP.

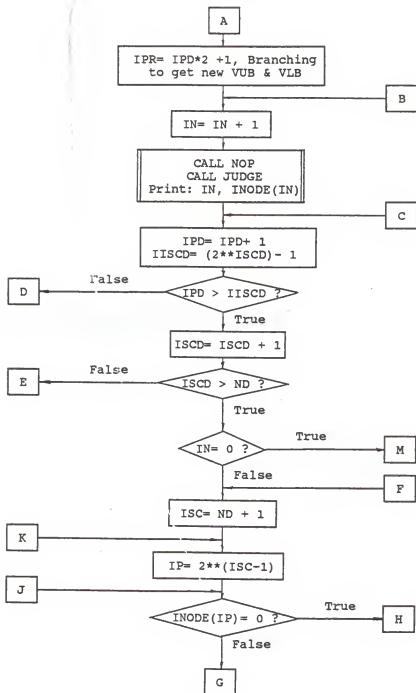


Figure 2.5--continued.

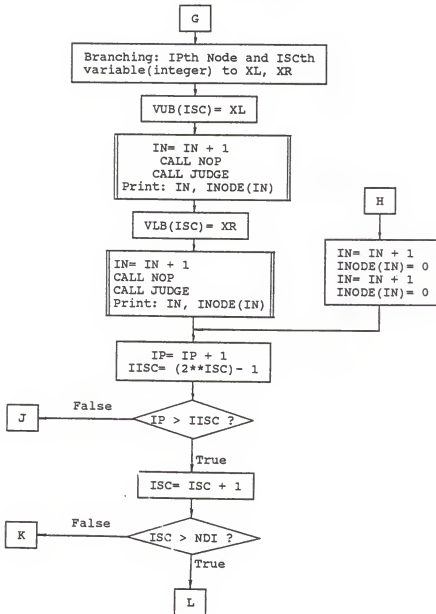


Figure 2.5--continued.

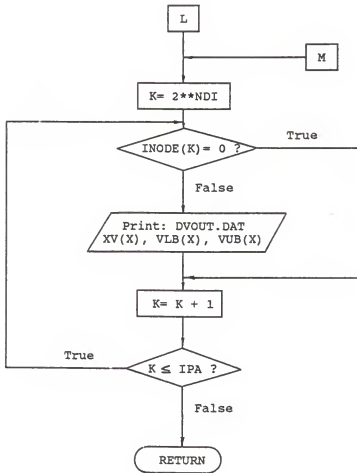


Figure 2.5--continued.

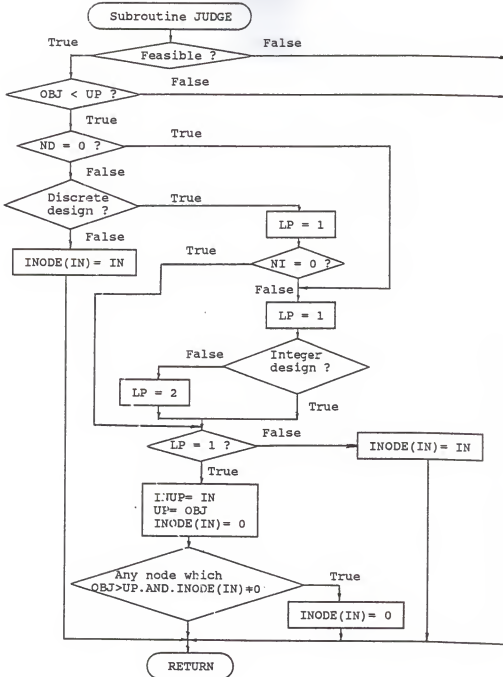


Figure 2.6 Flowchart for the subroutine JUDGE.



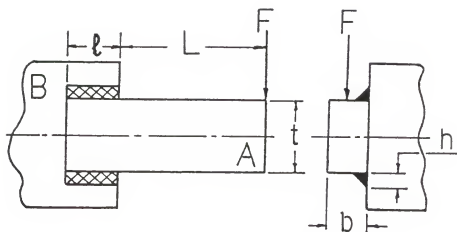


Figure 2.7 Configuration of the welded beam structure.

there are four design variables in the problem and these are the weld thickness  $h$ , the weld length  $\ell$ , and the bar thickness and breadth given by  $t$  and  $b$ , respectively. An optimal solution of the continuous problem was obtained as follows.

$$f(t,b,h,\ell)=2.38, \quad (t,b,h,\ell)=(8.29,0.24,0.24,6.22)$$

Here  $f(t,b,h,\ell)$  is the objective function. The problem was next modified in steps to create a series of mixed integer discrete problems.

Case A. The variables  $t$  and  $b$  were restricted to integer values and the following optimum design was obtained.

$$f(t,b,h,\ell)=5.45, \quad (t,b,h,\ell)=(5,1,0.727,2.52)$$

Case B. The variables  $t$  and  $b$  were restricted to assume discrete values, and in this problem, were considered integer multiples of 0.5. The optimum solution was obtained as follows.

$$f(t,b,h,\ell)=3.48, \quad (t,b,h,\ell)=(6.0,0.5,0.499,3.47)$$

It is worthwhile to note that this result is better than that reported in [23].

Case C. One additional modification was introduced in which the variables  $h$  and  $l$  were assigned as integers, and variables  $t$  and  $b$  were chosen as discrete variables as in Case B. The following optimum solution was obtained.

$$f(t,b,h,l)=5.67, \quad \{t,b,h,l\}=\{4.5,1.0,1,2\}$$

Each of the results shown above was obtained by starting from several initial estimates of the design variables, and one can reasonably expect these to be the global optima. The branch and bound tree structure for the special case of mixed integer and discrete variables (case C) is shown in Figure 2.8.

The branch and bound algorithm developed in this study was applied in the optimum design of composite laminated beam structures, for constraints on strength, displacement and natural frequencies. The beam structure and the applied concentrated and distributed loads are shown in Figure 2.9, with details of the geometrical configuration of the multilayered laminate shown in Figure 2.10. With reference to Figure 2.10, the depth of the beam can be described by three layers, with each layer containing  $N_1$ ,  $N_2$ , and  $N_3$  plies of thickness  $t$ . The fiber orientations in these layers is given by  $\theta_1$ ,  $\theta_2$ , and  $\theta_3$ , respectively. The beam structure was analyzed as a special case of a laminated

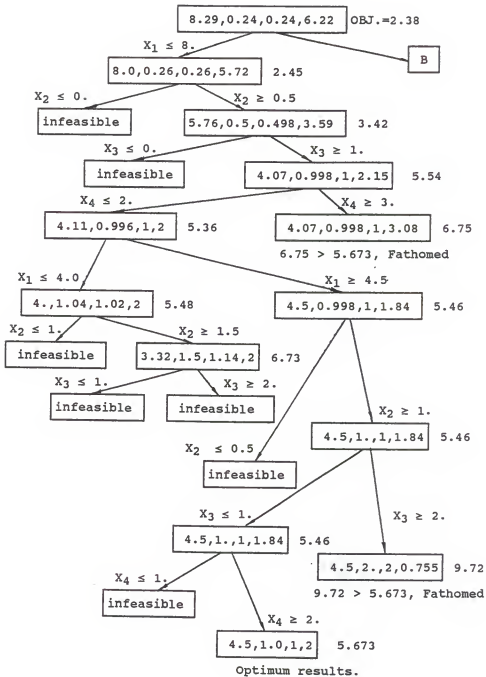


Figure 2.8 The binary tree structure obtained during branch and bound process in the design of the welded beam structure.

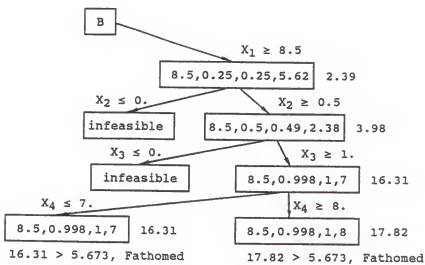


Figure 2.8--continued.

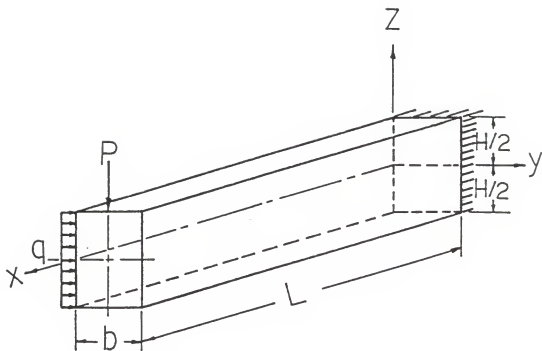


Figure 2.9 Configuration and loading of the composite laminated beam ( $P=6\text{ N}$ ,  $q=4/H\text{ N}$ ,  $L=250\text{ mm.}$ ,  $b=20\text{ mm.}$  ).

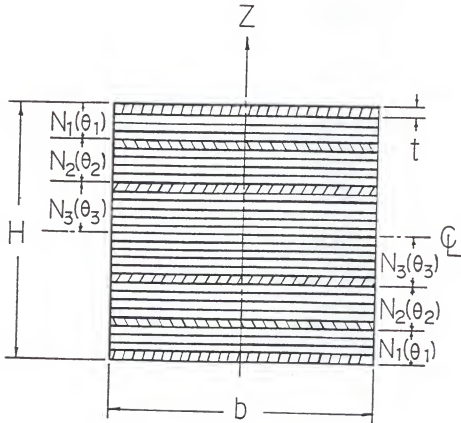


Figure 2.10 Geometrical configuration of the multilayered laminated structure.

composite plate [55], and the matrix equation relating the known force and moment resultants  $N$  and  $M$  to the strains and curvatures is written as follows [56].

$$\begin{Bmatrix} N \\ M \end{Bmatrix} = \begin{bmatrix} A & B \\ B & D \end{bmatrix} \begin{Bmatrix} \epsilon^o \\ \kappa \end{Bmatrix} \quad (2.23)$$

Here,  $A$ ,  $B$  and  $D$  are the extensional stiffness, coupling stiffness, and bending stiffness matrices, respectively. This study was restricted to symmetric laminates and  $B$  was therefore identically zero. The matrices  $A$  and  $D$  are functions of the geometrical layout of the composite including lamina thickness, fiber orientation and ply stacking sequence. They are additionally functions of engineering constants such as the longitudinal modulus  $E_L$ , transverse modulus  $E_T$ , the shear modulus  $G_{LT}$ , and the major Poisson ratio  $\nu_{LT}$ . These quantities are obtained in terms of fiber volume fraction and material properties by application of the rule of mixtures and Halpin-Tsai equations. The stresses in the individual lamina are dependent on the strains and curvatures as well.

In the optimum design problem, displacement and frequency constraints were introduced in addition to the strength constraints. The maximum tip deflection in the  $z$ -direction is denoted by  $\Delta_z$  and can be obtained as



$$\Delta z = \frac{PL^3}{3E_x^b I} \quad (2.24)$$

where  $I$  is the area moment of inertia of the whole cross section to the trace of the midplane;  $E_x^b$  was defined in [57] as the effective bending modulus of the laminated beam and has the following form

$$E_x^b = \frac{12}{H^3 D_{11}^*} \quad (2.25)$$

where  $D_{11}^*$  is the first element of the inverse of  $D$ . An estimate of the displacement in the  $y$  direction is obtained from

$$\Delta y = \frac{2q(N_1 + N_2 + N_3)tL^3}{3E_y I_y} \quad (2.26)$$

where  $I_y$  is the area moment of inertia relative to the  $z$ -axis and  $E_y$  is an equivalent extensional modulus that is obtained on the basis of the rule of mixtures as follows.

$$E_y = \sum_{i=1}^3 E_{yi} A_i / A, \quad (2.27)$$

where

$$A = bH, \quad A_i = 2N_i t b \quad (2.28)$$

The bending modulus of each of the three stacks of plies with identical fiber orientation angles can be obtained from the following equation.

$$\frac{1}{E_{yi}} = \frac{\sin^4 \theta_i}{E_L} + \frac{\cos^4 \theta_i}{E_T} + \frac{1}{4} \left( \frac{1}{G_{LT}} - \frac{2\nu_{LT}}{E_L} \right) \sin^2 2\theta_i \quad (2.29)$$

$i=1,2,3$

The natural frequencies of the beam were computed as follows

$$\omega_m = \frac{(\alpha_m L)^2}{2L^2} \frac{(E_x^b H^3)^{1/2}}{3\rho} \quad (2.30)$$

where the parameter  $\alpha_m$  depends on the boundary conditions of the beam problem. The numerical values of  $\alpha_m L$  for clamped-free beam, corresponding to the first and second mode of vibration are 1.875 and 4.694, respectively. The quantity  $\rho$  is defined in terms of a density of the laminated composite per unit length,  $\rho_0$ .

$$\rho = \int_{-H/2}^{H/2} \rho_0 dz \quad (2.31)$$

In this study, optimum designs for the prescribed constraints were obtained for five different composite materials. These ranged from high stiffness composites like graphite-epoxy to those with a high material damping like kevlar-epoxy. The material constants used in the study are listed in Table 2.1.

Table 2.1 Material Properties of the matrix and fibers.

Constants	Matrix	Fibers				
	Epoxy	Scotch (Glass)	Kev49 (Kevlar)	AS (Graphite)	T300	B4 (Boron)
$E_L$ (Gpa)	3.4	85.8	126.7	209.1	258.6	408.0
$E_T$ (Gpa)	3.4	85.6	7.0	15.5	18.2	409.8
$G_{LT}$ (Gpa)	1.47	35.5	3.0	160.5	36.7	185.3
$\nu_{LT}$	0.35	0.15	0.33	0.27	0.25	0.11
$\rho$ (Kg/m <sup>3</sup> )	1220	2600	1440	1750	1750	2600

The analysis presented in the preceding section clearly indicates that the design of the laminated composite depends upon material properties, and on geometry and configuration variables such as lamina thickness, number of plies, fiber orientation in each ply, and the volume fraction. These variables are of both the continuous and discrete type. The optimization problem is formulated as a multidimensional nonlinear programming problem with continuous, discrete and integer variables. The mathematical problem statement is as follows:

$$\text{Minimize } F = 2t (N_1 + N_2 + N_3) bL \rho_C g \quad (2.32)$$

Subject to

$$\Delta z \leq L/1000 \quad (2.33a)$$

$$\Delta y \leq L/1000 \quad (2.33b)$$

$$\omega_1 \geq 125 \text{ Hz} \quad (2.33c)$$

$$\omega_2 \geq 750 \text{ Hz} \quad (2.33d)$$

$$H \leq 2.5 \text{ cm} \quad (2.33e)$$

$$\left(\frac{\sigma_L}{\sigma}\right)_{LU}^2 - \left(\frac{\sigma_L}{\sigma}\right)_{LU} \left(\frac{\sigma_T}{\sigma}\right)_{LU} + \left(\frac{\sigma_T}{\sigma}\right)_{Tu}^2 + \left(\frac{\tau_{LT}}{\tau}\right)_{LTU}^2 \leq 1 \quad (2.33f)$$

In the above formulation, the width  $b$  and length  $L$  were chosen as 2 cm and 25 cm, respectively. The density of the composite  $\rho_c$  was defined in terms of fiber density  $\rho_f$ , matrix density  $\rho_m$ , and the fiber volume fraction  $V_f$  as follows.

$$\rho_c = \rho_f V_f + \rho_m (1 - V_f) \quad (2.34)$$

The thickness of each ply was considered to be a discrete variable, with admissible values selected from the following set.

$$t = (0.1, 0.125, 0.15, 0.175, 0.225, 0.275, 0.325, 0.375)$$

The number of plies in the three layers were considered as integer variables and allowed to assume values between 3 and 100. The fiber orientations were allowed to vary between  $-90$  and  $+90$  degrees and the volume fraction bounded between 0.5 and  $\pi/2\sqrt{3}$ . Both of these variables were assumed to be of the continuous type. The constraints defined in equations (2.33a-f) include tip displacements in  $z$  and  $y$  directions, lower bounds on the first and second frequencies, upper bound on the depth of the beam, and a strength constraint obtained on the basis of the Tsai-Hill failure theory [58]. In the strength constraint  $\sigma_{LU}$  and  $\sigma_{TU}$

are the allowable tensile strengths in the longitudinal and transverse directions, respectively, and  $\tau_{LTU}$  is the allowable shear strength. These allowable stress levels are listed in Table 2.2. For the optimization problem described above, the initial design was selected as follows.

$t=0.2$ mm	$N_1=5$	$N_2=30$	$N_3=14$
$\theta_1=10^\circ$	$\theta_2=40^\circ$	$\theta_3=-30^\circ$	$V_f=0.5$

The first set of results was obtained by treating all variables as continuous, and rounding to the nearest discrete or integer value. These results for the continuous and rounded variables are presented in Tables 2.3 and 2.4. The design obtained by rounding the continuous solution to the nearest discrete or integer solution gave poor estimates of the true optimal solution. As seen from the results, it sometimes yielded an infeasible solution. The discrete variable problem was then solved using the branch and bound algorithm developed in this chapter. The results obtained are presented in Table 2.5. Both sets of results described above were obtained for five different composite materials.

For the method where all variables were treated as continuous and the solution rounded to the nearest integer/discrete set, the optimum fiber orientations in the outer two layers were approximately aligned with the beam longitudinal axis. This provides the maximum stiffness in

Table 2.2 Allowable strengths of different fiber-epoxy composites. These strengths are the longitudinal tensile strength ( $\sigma_{LU}$ ), transverse tensile strength ( $\sigma_{TU}$ ), shear strength ( $\tau_{LTU}$ ), longitudinal compressive strength ( $\sigma'_{LU}$ ), and transverse compressive strength ( $\sigma'_{TU}$ ).

Constants	Fiber-Epoxy				
	Scotch (Glass)	Kev49 (Kevlar)	AS (Graphite)	T300	B4 (Boron)
$\sigma_{LU}$ (Mpa)	1062	1400	1447	1500	1260
$\sigma_{TU}$ (Mpa)	31	12	52	40	61
$\tau_{LTU}$ (Mpa)	72	34	93	68	67
$\sigma'_{LU}$ (Mpa)	610	235	1447	1500	2500
$\sigma'_{TU}$ (Mpa)	118	53	206	246	202

Table 2.3 Optimum results for the case where all variables are treated as continuous.

Fiber	Final design of all continuous variables								
	t (mm.)	N <sub>1</sub>	N <sub>2</sub>	N <sub>3</sub>	$\theta_1$	$\theta_2$ (degree)	$\theta_3$	V <sub>f</sub>	F (Newton)
Scotch	0.160	5.10	23.3	8.78	-8.67	1.74	-41.1	0.5	1.111
Kev49	0.146	8.86	12.2	8.00	-1.53	2.06	0.37	0.90	0.588
AS	0.140	4.89	17.5	7.42	0.34	-0.08	-20.4	0.57	0.623
T300	0.137	5.09	15.7	6.59	3.00	-0.29	-5.52	0.70	0.581
B4	0.136	3.98	16.7	6.54	8.17	0.50	11.8	0.5	0.687



Table 2.4 Final results obtained after rounding  $t$  and  $N_i$ , up or down, to nearest discrete or integer values.

Fibers	Rounding final design					
	$t$ (mm.)	$N_1$	$N_2$	$N_3$	$F$ (Newtons)	feasible?
Scotch	0.15	5	23	9	1.0341	No
Scotch	0.175	5	23	9	1.2065	Yes
Kev49	0.125	9	12	8	0.5031	No
Kev49	0.15	9	12	8	0.6037	Yes
AS	0.125	5	18	7	0.5580	No
AS	0.15	5	18	7	0.6696	Yes
T300	0.125	5	16	7	0.5440	No
T300	0.15	5	16	7	0.6529	Yes
B4	0.125	4	17	7	0.6521	No
B4	0.15	4	17	7	0.7826	Yes

Table 2.5 Optimum results for mixed integer and discrete design variables.

Fiber	Final optimum design								
	t (mm.)	N <sub>1</sub>	N <sub>2</sub>	N <sub>3</sub>	$\theta_1$	$\theta_2$ (degree)	$\theta_3$	V <sub>f</sub>	F (Newton)
Scotch	0.15	6	23	11	-5.2	5.86	-11.8	0.5	1.118
Kev49	0.15	9	12	8	-1.53	2.06	0.37	0.897	0.6037
AS	0.125	4	22	11	-13.0	10.1	-19.0	0.5	0.6689
T300	0.125	5	18	8	0.75	0.53	-11.0	0.61	0.5827
B4	0.125	3	18	10	-16.4	12.3	-16.1	0.5	0.722

bending in the z direction required to account for the displacement constraint. The largest variations of fiber orientations from the longitudinal direction were observed in the innermost layer, and this provided the necessary bending stiffness to satisfy the y-direction displacement constraint. When treated as a mixed integer-discrete variable problem by the branch and bound method, this effect was present to a lesser extent.

The weights of the final optimum designs obtained by the branch and bound approach were consistently lower than those obtained by the continuous approach. The optimal fiber volume fractions were at their lower bounds in most of the cases for which results were obtained. This was especially true for isotropic fibers such as Scotch Glass and Boron. In some anisotropic fibers, the optimal fiber volume ratios were higher. The final optimal weights were lower for the anisotropic fibers and this can be attributed to a lower fiber density.

## CHAPTER III

### MULTIOBJECTIVE OPTIMIZATION WITH MIXED INTEGER AND DISCRETE DESIGN VARIABLES

#### III.1 Introduction

Decisions in engineering design typically require allocation of resources to satisfy multiple, and frequently conflicting, requirements. Despite of the recognized multicriterion nature of most design problems, the bulk of research effort has been expended in developing efficient optimization methods for scalar objective function problems. In such an approach, one criterion is selected as the objective function, and the tradeoff amongst the remaining criteria is resolved by formulating appropriate design constraints. The apparent simplicity afforded by this method is attractive, but an effective case can be made against the use of such an approach. One can argue in favor of a method that deals with multiple criteria, stipulating "a 'natural' separation of criteria and constraints" in any design problem. Furthermore, a treatment of constraints as criteria provides a systematic approach to learn about the extent of the feasible set. In other words, when a multicriterion optimum is obtained, a tradeoff pattern emerges, wherein no criterion may be improved without

adversely affecting another. Furthermore, it is also known that the treatment of criteria as constraints does not yield the same optimum design as would be obtained when solving the optimum design problem as one possessing multiple objectives.

Multicriterion programming has emerged as a subject of special interest in mathematical nonlinear programming. One of the earliest efforts in this area may be attributed to an Italian economist Pareto, who in 1896 introduced the concept within the framework of welfare economics [24]. The ramifications of this work in optimization theory, operations research, and control theory were only recognized in the late 1960s. Applications of multicriteria optimization in engineering design have also been recognized. Baier [59,60] examined structural design problems in which weight and total energy in several loading conditions are considered as the design criteria. Pareto optimal designs of truss structures have been examined by Koski [29,61]. Numerous examples of design of mechanical structures have been presented, and works of Osyczka [62,63] and Rao and Hati [64] are typical of such applications. Another interesting application of a multiobjective design problem in viscoelasticity is presented in [65]. It does appear, however, that the full potential of multicriterion optimization has not been exploited in engineering design.

The present work proposes an approach for

multicriterion design that is derived from a global criterion approach [26], and is especially designed for problems where the design space could consist of continuous, discrete, or even integer design variables. A prerequisite to obtaining a solution to this problem is the availability of a methodology for solving mixed integer discrete optimization problems with a scalar objective function. An efficient approach for this class of problems was described in the previous chapter. A combination of the mixed-variable, nonlinear programming algorithm with a strategy to account for several objective criteria, is described in this chapter.

Subsequent sections of this chapter discuss the mathematical statement of the optimization problem. The optimization methodology is discussed with emphasis on formal proof of applicability, and the approach is implemented for purposes of concept verification. Optimum design results obtained for illustrative problems are also presented.

### III. 2 Multiobjective Optimum Design with Mixed Variables

The strategy used for multicriterion optimization in the present work can be broadly classified as belonging to a category of solution methods with no articulation of preference. In such an approach, also referred to as a

global criterion method [26], a metric function is formulated to represent the distance between the ideal solution and the optimum solution, and a minimization of this function results in the true optimum. For a problem involving  $m$  criterion functions, the ideal solution is an  $m$ -dimensional vector, the components of which are the optimum values of the individual criteria. These optimum values are obtained by considering each of the criterion separately in a scalar optimization problem. The application of the global criterion method is best illustrated by the sketch in Figure 3.1, which shows feasible and infeasible sectors in a space of two criterion functions. If the ideal solution,  $f^{id}(x)$ , were also feasible, there would be no additional effort required. However, this ideal solution is typically infeasible, and a feasible design closest to the ideal solution is sought. The Pareto optimal solution so obtained is such that the design variable vector cannot be altered without adverse effects on any one of the candidate criterion.

One can define a vector objective function  $f(x)$  dependent on the design variable vector  $x$ , where

$$f(x) = [f_1(x), f_2(x), \dots, f_i(x), \dots, f_k(x)]^T \quad (3.1)$$

$$X = [x_1, x_2, \dots, x_n]^T$$

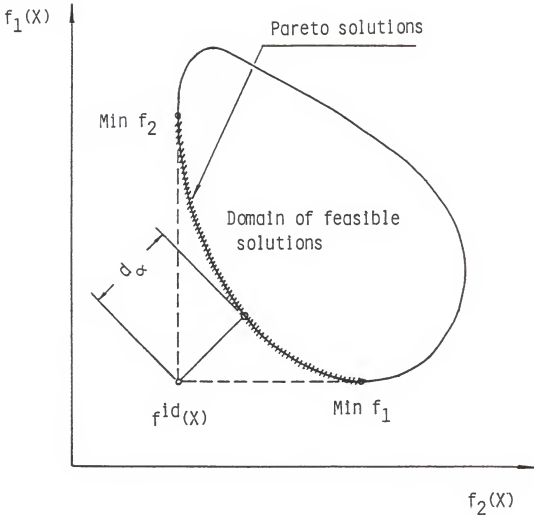


Figure 3.1 Graphical representation of Pareto (noninferior) solutions in a problem where two criteria must be minimized.



and  $f_i(X)$  is the  $i$ -th criterion function. If  $f_i^{id}(x)$  is the ideal solution corresponding to  $i$ -th criterion function, the optimal solution is obtained by minimizing a global criterion function of the form,

$$\text{Minimize } d_\alpha = \left[ \sum_{i=1}^k |f_i(x) - f_i^{id}(x)|^\alpha \right]^{1/\alpha} \quad (3.2)$$

subject to the prescribed design constraints

$$g_j(x) \leq 0, \quad j=1,2,\dots,r \quad (3.3)$$

$$h_k(x) = 0, \quad k=r+1,\dots,m \quad (3.4)$$

Here,  $d_\alpha$  is a distance metric with  $1 \leq \alpha \leq \infty$ . Typical choices of  $\alpha=1$  or  $\alpha=2$  have been used in the literature [66,67]. Numerical computations are better conditioned if a normalized objective function vector  $\tilde{f}(X)$  is used, where

$$\tilde{f}(x) = \left[ \tilde{f}_1(x), \tilde{f}_2(x), \dots, \tilde{f}_k(x) \right]^T \quad (3.5)$$

and the individual components of this vector function are obtained as follows.

$$\tilde{f}_i(x) = \frac{f_i(x) - \min f_i(x)}{\max f_i(x) - \min f_i(x)} \quad i = 1,2,\dots,k \quad (3.6)$$

In the present approach, a relative deviation metric is preferred over the absolute deviation represented by (3.2). The metric function to be minimized is stated as

$$\tilde{f}_i(x) = \frac{f_i(x) - f_i^{id}(x)}{f_i^{id}(x)} \quad i=1,2,\dots,k \quad (3.7)$$

and the summation in the metric function can be written as follows:

$$d_\alpha = \left[ \sum_{i=1}^k \left| \frac{f_i(x) - f_i^{id}(x)}{f_i^{id}(x)} \right|^\alpha \right]^{1/\alpha} \quad (3.8)$$

which in the limit of  $\alpha \rightarrow \infty$ , reduces to the following form.

$$d_\alpha = \max_i \left| \frac{f_i(x) - f_i^{id}(x)}{f_i^{id}(x)} \right| \quad i=1,2,\dots,k \quad (3.9)$$

Minimization of the metric function results in the commonly encountered min-max problem in multiobjective optimization. The mathematical statement of the optimization problem may therefore be written as follows.

$$\min_x \max_i \left| \frac{f_i(x) - f_i^{id}(x)}{f_i^{id}(x)} \right| \quad i=1,2,\dots,k \quad (3.10)$$

The solution to the above optimization problem yields the best compromise solution in which all criteria are considered equally important. Use of weighting coefficients can be introduced in conjunction with this method to rank the importance of the candidate criteria, and the min-max problem is restated as follows:

$$\min_x \max_i \omega_i \left| \frac{f_i(x) - f_i^{id}(x)}{f_i^{id}(x)} \right| \quad i = 1, 2, \dots, k \quad (3.11)$$

where  $\omega_i$  is the weighting coefficient representing the relative importance of the  $i$ -th criterion. It is usually assumed that

$$\sum_{i=1}^k \omega_i = 1 \quad (3.12)$$

In a situation where the design variable set is a mixture of continuous, integer, and discrete design variables, the choice of an ideal solution for use in the global criterion method is an important consideration. In the present work, the ideal solution was selected as the one obtained by treating all design variables as continuous. The mathematical basis for this selection is as follows.

First, a scalar variable  $\beta$  is introduced to facilitate the transformation of the min-max problem of equation (3.10) into an equivalent scalar optimization problem.

$$\text{Minimize } \beta \quad (3.13a)$$

subject to the following additional constraints:

$$\omega_i \left| \frac{f_i(x) - f_i^{id}(x)}{f_i^{id}(x)} \right| - \beta \leq 0 \quad i = 1, 2, \dots, k \quad (3.13b)$$

Since the first term in the left hand side of equation (3.13b) is always positive, the smallest value of  $\beta$  would be obtained in a situation when the equality is strictly satisfied.

$$\left| \frac{f_i(x)}{f_i^{id}(x)} - 1 \right| = \beta / \omega_i \quad i=1,2,\dots,k \quad (3.14)$$

It can be further argued that the ideal solution obtained by minimizing  $f_i(X)$  with all design variables treated as continuous, will always be smaller than or equal to the function value obtained by imposing discrete or integer requirements on some design variables.

Hence,

$$\frac{f_i(x)}{f_i^{id}(x)} \geq 1 \quad (3.15)$$

and equation (3.14) can be rearranged as follows.

$$f_i(x) = f_i^{id}(x) \left( 1 + \frac{\beta}{\omega_i} \right) \quad (3.16)$$

From equation (3.16) one can conclude that a smaller value of  $f_i^{id}(x)$  will minimize the function  $f_i(x)$  when scalar variable  $\beta$  is minimized. The ideal solution should therefore be obtained by treating all design variables as continuous.

### III.3 Illustrative Example

A flowchart for the algorithm described in the preceeding section is shown in Figure 3.2. The algorithm was first implemented in the design of a simply supported beam [63] shown in Figure 3.3. The objective of the design problem was to select the design variables  $x_1, x_2, x_3$ , and  $x_4$ , to minimize both the weight of the beam and its deflection at the mid span under the applied loads. The mathematical statement of the optimum design problem can be written as follows:

$$\text{Minimize} \quad (f_1, f_2)$$

where

$$f_1(x) = 2x_2x_4 + x_3(x_1 - 2x_4) \quad (\text{Volume}) \quad (3.17)$$

$$f_2(x) = PL^3/48EI \quad (\text{Central deflection}) \quad (3.18)$$

$$I = \{x_3(x_1 - 2x_4)^3 + 2x_2x_4[4x_4^2 + 3x_1(x_1 - 2x_4)]\}/12 \quad (3.19)$$

(Centroidal area moment of inertia at the cross section)

subject to the strength constraints

$$\frac{M_y}{Z_y} + \frac{M_z}{Z_z} \leq \sigma_b \quad (3.20)$$

Here  $P = 600$  kN,  $L = 200$  cm,  $E = 2 \times 10^4$  kN/cm<sup>2</sup>,  $\sigma_b = 16$  kN/cm<sup>2</sup> is the permissible bending stress,  $M_y$  and  $M_z$  are the maximal

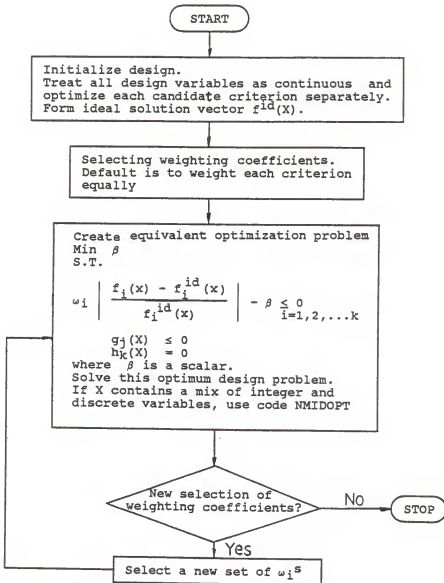


Figure 3.2 Flow diagram representation of multiobjective optimization combined with code NMIDOPT for mixed integer and discrete design variable problem.

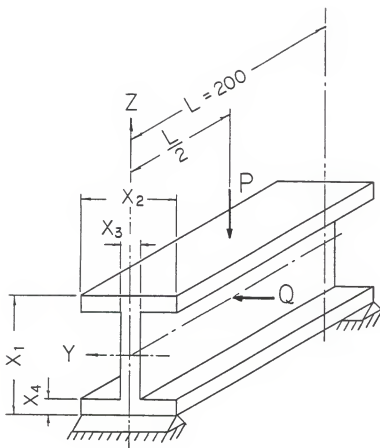


Figure 3.3 Definition of design variables and loading for the simply support I-beam.

bending moments in the y and z directions, respectively, and  $Z_y$  and  $Z_z$  are the section modulii. Additional side constraints are also imposed in the design problem.

$$10 \text{ cm} \leq x_1 \leq 80 \text{ cm} \quad (3.21a)$$

$$10 \text{ cm} \leq x_2 \leq 50 \text{ cm} \quad (3.21b)$$

$$0.9 \text{ cm} \leq x_3 \leq 5 \text{ cm} \quad (3.21c)$$

$$0.9 \text{ cm} \leq x_4 \leq 5 \text{ cm} \quad (3.21d)$$

A modified feasible usable search direction technique was used to obtain the separately attainable minimum of each component of the objective function as follows.

$$\begin{aligned} f_1^{id}(x_{(1)}) &= 127.443, & f_2^{id}(x_{(1)}) &= 0.05934 \\ (x_{(1)})^{id} &= (61.78, 40.81, 0.9, 0.9) \end{aligned}$$

$$\begin{aligned} f_1^{id}(x_{(2)}) &= 850.0, & f_2^{id}(x_{(2)}) &= 0.005903 \\ (x_{(2)})^{id} &= (80.0, 50.0, 5.0, 5.0) \end{aligned}$$

Hence, the ideal solution vector can be written as

$$f^{id} = (127.443, 0.005903)$$

Using a weighting coefficient strategy, one can obtain a set of Pareto solutions as illustrated in Figure 3.4.

All points in the interior of the feasible space represent inferior solutions, as one can always find a point on the boundary for which both criteria can be



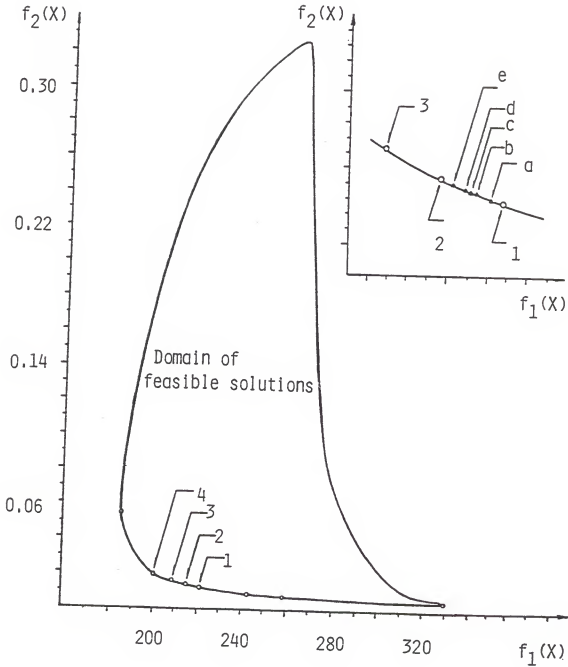


Figure 3.4 Graphical representation of the Pareto (noninferior) set of solutions for the I-Beam problem.

simultaneously improved. Points on the boundary, however, belong to a noninferior or a Pareto set. A subset of these Pareto optimal solutions is presented in Table 3.1. If more alternatives are required between points 1 and 2, the weighting coefficients are adjusted to assume values between 0.45 and 0.55. Representative alternative solutions are indicated by points a,b,c,d and e in Figure 3.4.

The problem was then modified to introduce discrete and integer design variables. Variables  $x_3$  and  $x_4$  were chosen to be of the discrete type, assuming values between 0.9 and 5.0, in increments of 0.1. Another modification involved treating  $x_3$  and  $x_4$  as variables of the integer and discrete type, respectively. The optimum results obtained are summarized in Table 3.2.

The algorithm developed above was implemented in a design of a cantilever composite laminate beam. The beam and the applied concentrated and distributed loads are shown in Figure 2.9 of Chapter II, with details of the geometrical configuration of the multilayered laminate shown in Figure 2.10 of Chapter II. The beam structure was analyzed as a special case of a symmetric laminated composite plate and the details of the analysis are available in Chapter II. The design of the laminated composite depends upon material properties, and on the geometry and configuration variables such as lamina thickness, number of plies, fiber orientation in each ply, and the volume fraction. These variables are

Table 3.1 A representative subset of Pareto (noninferior) solutions for the I-Beam design problem.

Case No	Weighting Coef. ( $\omega_1, \omega_2$ )	Design Variables $X = (x_1, x_2, x_3, x_4)$	Optimum Objective $f(X) = (f_1, f_2)$
1	(0.45, 0.55)	(79.99, 49.99, 0.9, 2.39)	(307.53, 0.0127)
2	(0.55, 0.45)	(80.0, 50.0, 0.9, 2.083)	(276.55, 0.0143)
3	(0.65, 0.35)	(79.99, 50.0, 0.9, 1.791)	(247.88, 0.0163)
4	(0.80, 0.20)	(80.0, 39.79, 0.9, 1.725)	(206.14, 0.0205)

Table 3.2 Optimum results for the I-Beam problem for three different variable types. Weighting coefficient  $\omega_i=0.5$  is used.

Case Description $X = (x_1, x_2, x_3, x_4)$	Objective Function $f(X) = (f_1, f_2)$
A. All real continuous variables. $X = (79.99, 49.99, 0.9, 2.235)$	(291.43, 0.01351)
B. $x_3$ and $x_4$ are discrete type. $X = (80.0, 48.69, 0.9, 2.30)$	(291.85, 0.01350)
C. $x_3$ is integer, $x_4$ is discrete type. $X = (80.0, 49.72, 1, 2.20)$	(294.38, 0.01362)

of both the continuous and discrete type. With reference to Figure 2.10 of Chapter II, the depth of the beam can be described by three layers, with each layer containing  $N_1$ ,  $N_2$ , and  $N_3$  plies of thickness  $t$ . The fiber orientations in these layers is given by  $\theta_1$ ,  $\theta_2$ , and  $\theta_3$ , respectively. In this problem, we need to minimize the total structural weight as well as the tip deflection in the  $z$  direction.

The optimization problem is formulated as a multidimensional nonlinear programming problem with continuous, discrete and integer variables. The mathematical problem statement is as follows.

Minimize  $(F, \Delta_z)$

where

$$F = 2t (N_1 + N_2 + N_3) bL \rho_C g \quad (3.22)$$

$$\Delta_z = PL^3 / 3E_X bI \quad (3.23)$$

Subject to :

$$\Delta_y \leq L/1000 \quad (3.24a)$$

$$\omega_1 \geq 125 \text{ Hz} \quad (3.24b)$$

$$\omega_2 \geq 750 \text{ Hz} \quad (3.24c)$$

$$H \leq 2.5 \text{ cm} \quad (3.24d)$$

$$\left(\frac{\sigma_L}{\sigma_{LU}}\right)^2 - \left(\frac{\sigma_L}{\sigma_{LU}}\right)\left(\frac{\sigma_T}{\sigma_{LU}}\right) + \left(\frac{\sigma_T}{\sigma_{TU}}\right)^2 + \left(\frac{\tau_{LT}}{\tau_{LTU}}\right)^2 \leq 1 \quad (3.24e)$$

Here  $F$  is the structural weight and  $\Delta_z$  is the tip deflection in the  $z$  direction;  $I$  is the area moment of inertia of the whole cross section relative to the trace of the midplane, and  $E_X^b$  is defined in [57] as the effective beam modulus of the laminated beam.

In the above formulation, the width  $b$  and length  $L$  were chosen as 2 cm and 25 cm, respectively. The density of the composite  $\rho_C$  was defined in Eqn. (2.34) of chapter II. The thickness of each ply was considered to be a discrete variable, with admissible values selected from the following set.

$$t = \{0.1, 0.125, 0.15, 0.175, 0.225, 0.275, 0.325, 0.375\}$$

The side constraints such as number of plies in each layer and the fiber orientation are the same as in the previous chapter. The allowable stress levels and initial design are also the same as in chapter II.

The ideal solution was obtained by treating all design variables as continuous, and for two representative fiber materials, was as follows.

$f_{id} = (0.93095 \text{ N}, 0.01548 \text{ mm})$  for Scotch glass

$f_{id} = (0.34428 \text{ N}, 0.00633 \text{ mm})$  for T300 graphite

These ideal solutions were used in conjunction with the weighting coefficient technique to generate a series of Pareto optimal solutions for different weight coefficients. Table 3.3 shows representative results for a Scotch-Epoxy composite structure for both continuous and mixed type design variables. Optimum design variables for five kinds of fibers in the case when both criteria are equally weighted, are shown in Table 3.4.

One can compare the results of the previous chapter and the present section, and generally see the significant differences in the designs. The reason for these differences is that when we work with constraints, the results are always in the feasible domain. However, a systematic application of the multicriterion approach results in designs which are on the boundaries of the feasible set.

Table 3.3 A set of Pareto optimal solutions for the Scotch glass composite structure.

Weight Coeff.	Weight (Newtons)	z-deflection (mm.)	Variable type
(0.30, 0.70)	2.3698	0.02582	(All continuous)
(0.30, 0.70)	2.4365	0.02674	(Mixed type)
(0.50, 0.50)	2.1276	0.03584	(All continuous)
(0.50, 0.50)	2.139	0.03585	(Mixed type)
(0.70, 0.30)	1.8322	0.05602	(All continuous)
(0.70, 0.30)	1.889	0.05177	(Mixed type)



Table 3.4 Multiobjective optimum results of mixed integer and discrete design variables for five different composite structures.

Fiber	Final optimum design									
	t (mm.)	N <sub>1</sub>	N <sub>2</sub>	N <sub>3</sub>	$\theta_1$	$\theta_2$ (degree)	$\theta_3$	V <sub>f</sub>	F (Newtons)	$\Delta z$ (mm.)
Scotch	0.225	6	24	21	-8.9	6.1	-11.7	0.5	2.139	0.0358
Kev49	0.100	11	18	50	0.57	-4.28	3.37	0.9	1.097	0.0420
AS	0.225	4	15	18	-3.5	0.	-2.36	0.85	1.36	0.0230
T 300	0.125	7	39	19	-1.1	0.	-4.81	0.72	1.273	0.0234
B4	0.175	3	29	18	-4.53	0.	5.64	0.56	1.705	0.0153

## CHAPTER IV

### OPTIMUM SYNTHESIS OF SHORT FIBER COMPOSITES FOR IMPROVED INTERNAL MATERIAL DAMPING

#### IV.1 Introduction

The increased application of composite materials in structures that are subjected to dynamic loads, has introduced stringent requirements on the dynamic characteristics of these materials. In addition to the requirements on stiffness, strength, density, and coefficient of thermal expansion, the dynamic-load environment introduces the need to tailor the internal material damping characteristics.

The damping properties of continuous fiber composites have been the subject of considerable research. References [68-71] are typical of such studies and range in scope from analytical estimates to experimental observations. Glass and graphite reinforced polymer matrix composites exhibit anisotropic, linear viscoelastic behavior. The principal mechanism for damping in these composites is the viscoelastic energy dissipation that occurs in the polymer matrix. Experimental investigations [38,72] indicate that the damping in composites reinforced by discontinuous fibers is in general greater than that in continuous fiber composites. Sun and Wu [73] attribute this to the stress

concentration effects present at the fiber ends, which facilitate the transfer and dissipation of energy in the viscoelastic polymer matrix.

The first attempt to tailor the damping properties of basic composite structures can be traced to an effort due to Plunkett and Lee [41]. Several models have been proposed for predicting the damping in short fiber reinforced composites. Reference [37] discusses a formulation for obtaining the internal damping for a case in which the load is applied parallel to the fiber direction. The elastic-viscoelastic correspondence principle is used in conjunction with both an energy formulation and a force balance procedure to obtain the analytical models. Results obtained in the analysis are shown to be in good agreement with experimental data.

Sun and his co-workers have developed theoretical relationships for the material damping of aligned short fiber-reinforced polymer matrix composites under off-axis loading [40]. They developed relations for the loss and storage modulus in terms of fiber aspect ratio, loading angle, stiffness of the fiber and matrix materials, the volume fraction and the damping properties of the fiber and matrix materials. They also conducted parametric studies to examine the variation of the damping with the fiber aspect ratio and the loading angle, to determine optimum values of these parameters for maximum internal damping.

Parametric studies of the type described above are invaluable in design synthesis procedures. They have, however, been shown to yield suboptimal results. The present paper proposes a design synthesis approach based on formal multidimensional optimization that circumvents some of these problems. The approach used is one in which the extensional loss factor of a representative volume element is maximized subject to constraints on the element mass and stiffness characteristics. Two distinct analysis models, one that uses Cox's shear-lag theory [39,74], and another based on an advanced shear lag theory that allows for the matrix to partially sustain extensional loads [75], are used in the present work. Subsequent sections discuss these analytical models and their adaptation in an optimum synthesis environment.

#### IV.2 Analytical Estimates of Damping by Cox's Shear-Lag Model

A force balance approach was used with two distinct models to obtain expressions for damping in short fiber composites. The first method is similar to [39], and is summarized here for completeness. A representative volume element, shown in Figure 4.1, describes the geometrical relationship between the fiber and matrix materials. Short fibers of length  $s$  and diameter  $d$  are embedded in a matrix element of length  $s+p$  and diameter  $D$ . The ratio  $s/d$  is referred to as the fiber aspect ratio and  $p/s$  denotes the

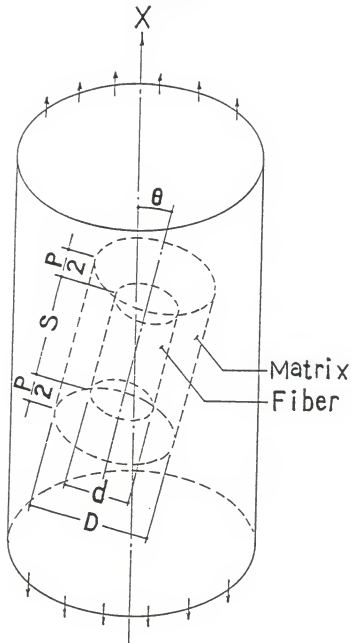


Figure 4.1 Representative volume element for off-axis loading.

discontinuity ratio.

The element is subjected to a longitudinal strain  $\epsilon_L$ . The rate of transfer of the load from the fiber to the matrix can be established from the relation between the displacement of the fiber and matrix materials, and is presented in [74]. The latter, referred to as the Cox's shear lag analysis, permits one to write the average stress  $\sigma_a$  in a fiber of length  $s$  as

$$\sigma_a = \frac{2}{s} \int_0^{s/2} \sigma_f dx = \epsilon_f E_f \left( 1 - \frac{\tanh(\beta s/2)}{\beta s/2} \right) \quad (4.1)$$

where  $\sigma_f$  is the stress in the fiber and  $\beta$  is defined by the following expression.

$$\beta^2 = \frac{G_m}{E_f} \frac{2}{d^2 \ln(D/d)} \quad (4.2)$$

$E_f$  and  $\epsilon_f$  are the extensional modulus of the fiber and the fiber strain, respectively. For static equilibrium under an applied load, an expression for the stress  $\sigma_c$  in the composite specimen can be written as

$$\sigma_c = E_L \epsilon_L = \sigma_a V_f + \sigma_m V_m \quad (4.3)$$

where  $V_f$  and  $V_m$  are the fiber volume fractions for the fiber and matrix materials, respectively. By substituting the value for the average fiber stress from Eqn. (4.1) and  $E_m \epsilon_m$  for the matrix stress  $\sigma_m$ , and assuming equal axial strain in the fiber and matrix materials, one can write an expression

for the elastic modulus in the longitudinal direction  $E_L$ , as follows.

$$E_L = E_f \left\{ 1 - \frac{\tanh(\beta s/2)}{\beta s/2} \right\} V_f + E_m V_m \quad (4.4)$$

In the present analysis, both fiber and matrix material were assumed to be viscoelastic. The elastic-viscoelastic correspondence principle can be used to define the extensional and shear moduli as the following complex quantities.

$$E_X^* = E_X' + iE_X'' \quad (4.5)$$

$$E_f^* = E_f' + iE_f'' \quad (4.6)$$

$$E_m^* = E_m' + iE_m'' \quad (4.7)$$

$$G_m^* = G_m' + iG_m'' \quad (4.8)$$

Subscripts 'f' and 'm' denote fiber and matrix materials. The prime and double prime quantities represent the storage and loss moduli, respectively. The ratio  $E_X''/E_X'$  is the loss factor and is a measure of the internal damping. With these definitions, the complex representation of equation (4.4) is written as follows.

$$E_L^* = E_f^* \left\{ 1 - \frac{\tanh(\beta^* s/2)}{\beta^* s/2} \right\} V_f + E_m^* (1 - V_f) \quad (4.9)$$

Here, the parameter  $\beta^*$ s depends on the geometrical arrangement of the fibers in the matrix. For square packing geometry, we have

$$\beta^*_{s=4} = 4 \left( \frac{\pi}{d} \right) \left( \frac{G_m^*}{E_f^* \ln \frac{\pi}{4V_f}} \right)^{0.5} \quad (4.10)$$

and for hexagonal packing geometry

$$\beta^*_{s=4} = 4 \left( \frac{\pi}{d} \right) \left( \frac{G_m^*}{E_f^* \ln \frac{\pi}{2\sqrt{3}V_f}} \right)^{0.5} \quad (4.11)$$

The Halpin-Tsai equations [56], in conjunction with the rule of mixtures, allows one to write expressions for the transverse modulus  $E_T^*$  and the in-plane shear modulus  $G_{LT}^*$ ,

$$E_T^* = E_m^* \left( \frac{1 + 2\eta_1 V_f}{1 - \eta_1 V_f} \right) \quad (4.12)$$

$$G_{LT}^* = G_m^* \left( \frac{1 + \eta_2 V_f}{1 - \eta_2 V_f} \right) \quad (4.13)$$

where

$$\eta_1 = (E_f^*/E_m^* - 1) / (E_f^*/E_m^* + 2) \quad (4.14)$$

and

$$\eta_2 = (G_f^*/G_m^* - 1) / (G_f^*/G_m^* + 1) \quad (4.15)$$

Furthermore, the Poisson ratio can be expressed as follows.



$$\nu_{LT} = \nu_f \nu_f + \nu_m (1 - \nu_f) \quad (4.16)$$

Here,  $\nu_f$  and  $\nu_m$  are the Poisson ratio for the fiber and matrix materials, respectively. With the above definitions, the modulus  $E_X^*$  assumes the following form.

$$\frac{1}{E_X^*} = \frac{1}{E_X' + iE_X''} = \frac{\cos^4 \theta}{E_L^*} + \frac{\sin^4 \theta}{E_T^*} + \left( \frac{1}{G_{LT}^*} - \frac{2\nu_{LT}}{E_L^*} \right) \sin^2 \theta \cos^2 \theta \quad (4.17)$$

Equation (4.17) can be separated into real and imaginary parts to yield values of the storage and loss moduli. As defined before, the loss factor is then expressed as follows.

$$\eta_X = E_X'' / E_X' \quad (4.18)$$

The shear loss factor is defined as the ratio of the storage to loss components of the shear modulus, where the latter are obtained from the expression shown below.

$$\begin{aligned} \frac{1}{G_{XY}^*} = \frac{1}{G_{XY}' + iG_{XY}''} &= \frac{1}{E_L^*} + \frac{2\nu_{LT}}{E_T^*} + \frac{1}{E_T^*} \\ &- \left( \frac{1}{E_L^*} + \frac{2\nu_{LT}}{E_L^*} + \frac{1}{E_T^*} - \frac{1}{G_{LT}^*} \right) \cos^2 2\theta \end{aligned} \quad (4.19)$$

A systematic parametric study of glass-epoxy and graphite-epoxy composites was conducted to examine the variation of damping with the volume fraction, fiber aspect ratio and loading angle. All material properties are summarized in Table 4.1. Representative curves for volume fractions of 0.5 and 0.65, and square and hexagonal packing geometry, are shown in Figures 4.2 and 4.3. Similar variations were also obtained for the extensional and shear moduli, and are depicted in Figures 4.4 and 4.5. Optimum values of loading angles can be deduced from these curves for various fiber aspect ratios. It is evident that a comprehensive study of all possible combinations of parameters would be extremely cumbersome. The approach of treating the problem as a multidimensional optimization problem is an attractive alternative.

#### IV.3 Formulation of an Advanced Shear-Lag Model to Obtain Internal Damping

A two-dimensional aligned short fiber arrangement in the matrix material is shown in Figure 4.6, from which a representative three-fiber model of the form shown in Figure 4.6--continued can be extracted. The matrix material between the fibers is considered an extension of the fiber with a different modulus. The free body diagram of the middle fiber is shown in Figure 4.7.

The following differential equations are obtained from force equilibrium considerations.

Table 4.1 Material properties of the matrix and fiber materials.

Constants	Matrix	Fibers	
	epoxy	glass	graphite
$E_L$ (Gpa)	3.4	72.4	228.
$E_T$ (Gpa)	3.4	72.4	13.8
$G_{LT}$ (Gpa)	1.4	$E_L/[2(1+\nu)]$	27.6
$\nu_{LT}$	0.4	0.2	0.16
$\eta$	0.015	0.0014	0.0014
$\eta_G$	0.018	—	—
$\rho$ (Kg/m <sup>3</sup> )	1220	2539	1760

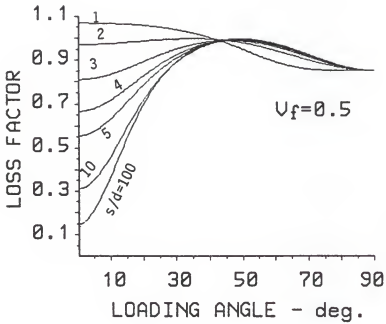


Figure 4.2 Characteristic curves for Glass Epoxy composite of  $V_f = 0.5$  (Square packing geometry).

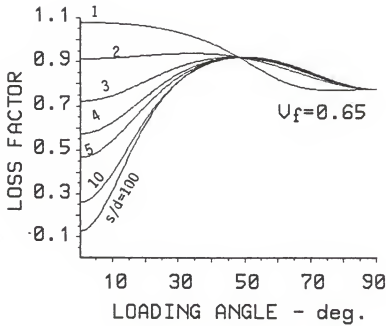


Figure 4.3 Characteristic curves for Glass Epoxy Composite of  $V_f=0.65$  (Hexagonal packing geometry).

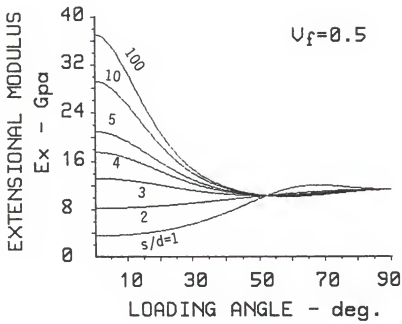


Figure 4.4 Extensional modulus for Glass Epoxy composite of  $V_f = 0.5$  (Square packing geometry).

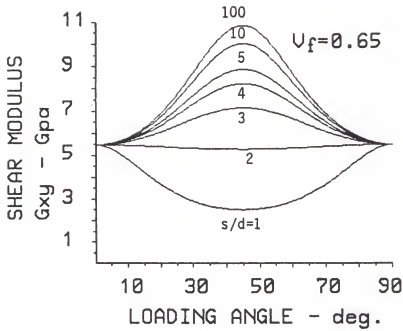


Figure 4.5 Shear modulus for Glass Epoxy composite of  $V_f = 0.65$  (Square packing geometry).

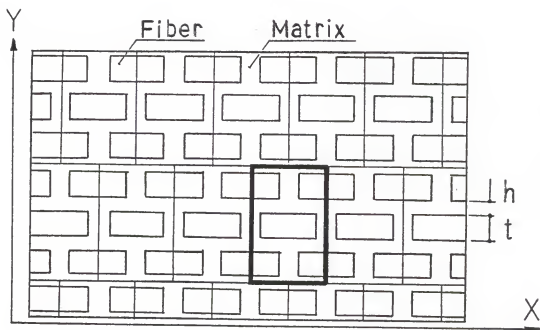


Figure 4.6 A 2-D short fiber arrangement in matrix material





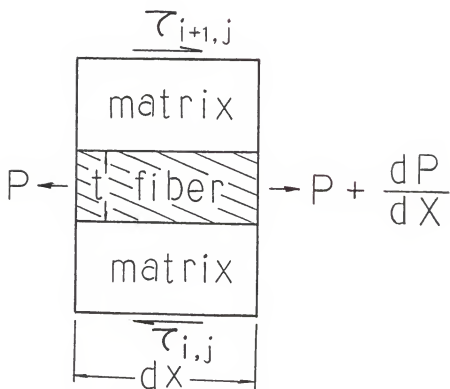


Figure 4.7 Free body diagram of middle fiber.

$$dP_{1j}/dx + r_{1j} = 0 \quad (4.20)$$

$$dP_{2j}/dx + r_{2j} - r_{1j} = 0 \quad (4.21)$$

$$dP_{3j}/dx - r_{2j} = 0 \quad (4.22)$$

Here  $P_{ij}$  and  $r_{ij}$  are the axial force per unit thickness and interfacial shear stress in the  $i$ -th fiber and  $j$ -th region, respectively. The normal fiber stress and the interfacial shear stress can be written in terms of a displacement  $u_{ij}$  as follows:

$$\sigma_{ij} = E_{ij} du_{ij}/dx \quad (4.23)$$

$$r_{ij} = G_m (u_{i+1j} - u_{ij})/h \quad (4.24)$$

where  $E_{ij}$  is the Young's modulus of region  $ij$ , and  $G_m$  is the shear modulus of the matrix material. Using conditions of symmetry and continuity of displacements and stresses, a solution for the axial load variation in the composite  $P_{ij}$ , Eqns. (4.25)-(4.28), is obtained as a function of nondimensional spatial location  $\xi=x/t$  and the ratio of the matrix and fiber tensile moduli  $k=E_m/E_f$ .

$$P_{21} = \frac{3 P_0}{(1+2k)} \left( 1 - \frac{8k\lambda_1 G(1-k) \cosh \lambda_1 \xi}{3 F} \right) \quad (4.25)$$

$$P_{22} = P_0 \left( 1 + \frac{2(1-k)}{(1+2k)} \cosh \lambda_2 (\xi - \xi_2) \left( 1 - \frac{4GH}{F} \right) \right) \quad (4.26)$$

$$P_{32} = P_{12} = P_0 \left( 1 - \frac{(1-k)}{(1+2k)} \cosh \lambda_2 (\xi - \xi_2) \left( 1 - \frac{4GH}{F} \right) \right) \quad (4.27)$$

$$P_{33} = P_{13} = \frac{3 P_0}{(2+k)} \left( 1 + \frac{\lambda_3 k (1-k) \cosh \lambda_3 (\xi_1 - \xi)}{\lambda_2 (1+2k) \sinh \lambda_3 (\xi_3 - \xi_0)} \sinh \lambda_2 (\xi_0 - \xi_2) \right. \\ \left. \cdot \left( 1 - \frac{4GW}{F} \right) \right) \quad (4.28)$$

where

$$F = (2+k) \sinh \lambda_3 (\xi_1 - \xi_0) [4k \lambda_1 \lambda_2 \cosh \lambda_1 \xi_2 \cosh \lambda_2 (\xi_0 - \xi_2) \\ + \frac{4(1+3k) \lambda_2^2}{3} \sinh \lambda_1 \xi_2 \sinh \lambda_2 (\xi_0 - \xi_2)] + [12k \lambda_1^2 \lambda_3 \cosh \lambda_1 \xi_2 \cdot \\ \sinh \lambda_2 (\xi_0 - \xi_2) + 4k(1+3k) \lambda_2 \lambda_3 \sinh \lambda_1 \xi_2 \cosh \lambda_2 (\xi_0 - \xi_2)] \cdot \\ \cosh \lambda_3 (\xi_1 - \xi_0) \quad (4.29)$$

$$G = \lambda_2 \sinh \lambda_3 (\xi_1 - \xi_0) [1 + 2k + (2+k) \cosh \lambda_2 (\xi_0 - \xi_2)] + \\ 3k \lambda_3 \sinh \lambda_2 (\xi_0 - \xi_2) \cosh \lambda_3 (\xi_1 - \xi_0) \quad (4.30)$$

$$H = \frac{\lambda_2 (1+3k)}{3} \sinh \lambda_1 \xi_2 \tanh \lambda_2 (\xi - \xi_2) + \lambda_1 k \cosh \lambda_1 \xi_2 \quad (4.31)$$

$$W = \frac{\lambda_2 (1+3k)}{3} \sinh \lambda_1 \xi_2 \coth \lambda_2 (\xi_0 - \xi_2) + \lambda_1 k \cosh \lambda_1 \xi_2 \quad (4.32)$$

$\lambda_j$  is expressed as

$$\lambda_j = \left( \frac{\alpha_{2j} + 2\alpha_{3j}}{\alpha_{2j} \alpha_{3j}} \right)^{0.5} \quad (4.33)$$

and

$$\alpha_{ij} = E_{ij} h / Gt. \quad (4.34)$$

The load distribution (or stress distribution) in the middle short fiber and in the matrix material between the fibers for the three fiber model for selected values of  $k=E_m/E_f$  and  $G_m/E_m=14/34$ , is shown in Figure 4.8. For  $k$  close to zero, one observes the expected zero loads at the fiber end as would also be predicted by Cox's analysis. A similar trend in the outer fiber and matrix is observed in Figure 4.9.

The average axial force can be obtained by integrating the force expressions  $P_{ij}(\xi, k)$  over the fiber length. Expressions for these average forces are as follows.

$$\bar{P}_{21} = \frac{3 P_0}{1+2k} \left\{ 1 - \frac{16 G}{3 F} \frac{k \lambda_1 (1-k) \sinh(\Sigma p/2)}{\Sigma p} \right\} \quad (4.35)$$

$$\bar{P}_{22} = P_0 \left\{ 1 + \frac{4(1-k)}{\Gamma(s-p)(1+2k)} \sinh \frac{\Gamma}{2} (s-p) \left( 1 - \frac{4GY}{F} \right) \right\} \quad (4.36)$$

$$\bar{P}_{32} = \bar{P}_{12} = P_0 \left\{ 1 - \frac{2(1-k)}{\Gamma(s-p)(1+2k)} \sinh \frac{\Gamma}{2} (s-p) \left( 1 - \frac{4GY}{F} \right) \right\} \quad (4.37)$$

$$\bar{P}_{33} = \bar{P}_{13} = \frac{3 P_0}{(2+k)} \left\{ 1 + \frac{2 \lambda_3 k (1-k)}{\Lambda p \lambda_2 (1+2k)} \left[ \sinh \frac{\Gamma}{2} (s-p) - \frac{4GW}{F} \right] \right\} \quad (4.38)$$

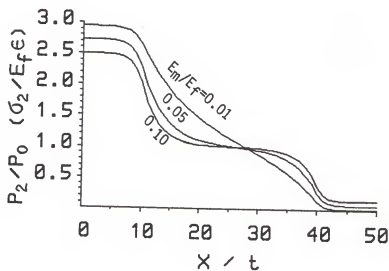
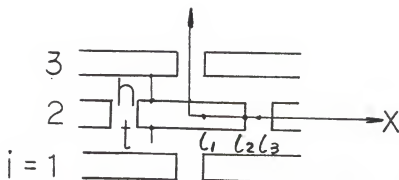


Figure 4.8 Load distribution along middle fiber and matrix.

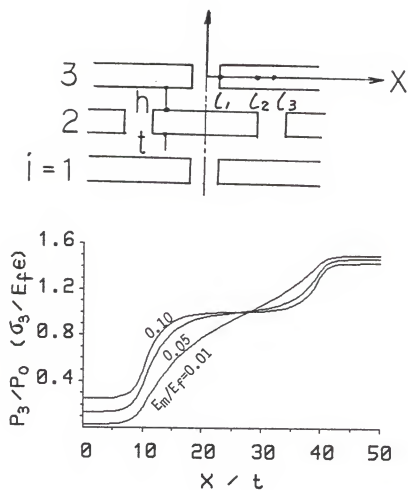


Figure 4.9 Load distribution along outer fiber and matrix.

where

$$\gamma = \frac{\lambda_2 (1+3k) \sinh \frac{\Sigma p}{2} [\cosh \frac{\Gamma}{2} (s-p) - 1]}{3 \sinh \frac{\Gamma}{2} (s-p)} + \lambda_1 k \cosh \frac{\Sigma p}{2} \quad (4.39)$$

and

$$\Sigma = \frac{\lambda_1}{d} = \frac{1}{d} \left( \frac{G_m (E_f + 2E_m)}{E_f E_m \sqrt{\frac{\pi}{4 V_f} (1+p/s) - 1}} \right)^{0.5} \quad (4.40)$$

$$\Gamma = \frac{\lambda_2}{d} = \frac{1}{d} \left( \frac{3 G_m}{E_f \sqrt{\frac{\pi}{4 V_f} (1+p/s) - 1}} \right)^{0.5} \quad (4.41)$$

$$\Lambda = \frac{\lambda_3}{d} = \frac{1}{d} \left( \frac{G_m (E_m + 2E_f)}{E_m E_f \sqrt{\frac{\pi}{4 V_f} (1+p/s) - 1}} \right)^{0.5} \quad (4.42)$$

Further, one can denote the average stress in each region of fiber by  $\bar{\sigma}_{21}$ ,  $\bar{\sigma}_{22}$ ,  $\bar{\sigma}_{32}$  and  $\bar{\sigma}_{33}$ . The average stress in a representative fiber length 's' can be obtained in terms of these quantities through a simple averaging formula as follows.

$$\sigma_a = \frac{1}{3s} \{ \bar{\sigma}_{21} p + \bar{\sigma}_{22} (s-p) + 2[\bar{\sigma}_{32} (s-p) + \bar{\sigma}_{33} p] \} \quad (4.43)$$

For static equilibrium under applied load, an expression for the stress,  $\sigma_c$ , in the composite specimen can be obtained from the following modified rule-of-mixture relationship



$$\sigma_c = \sigma_a V_f (1 + p/s) + \sigma_m [1 - V_f (1 + p/s)] \quad (4.44)$$

where  $V_f$  is the fiber volume fraction of the representative volume element. By substituting the value for the average fiber stress from equation (4.43), and  $E_m G_m$  for the matrix stress  $\sigma_m$  into equation (4.44), and assuming equal axial strain in fiber and matrix material, one can write an expression for the longitudinal modulus,  $E_c$ , of the representative volume element of composite of fiber length as follows.

$$E_c = E_f V_f (1 + p/s) \left[ 1 - \frac{\tanh(\beta s/2)}{\beta s/2} \right] + E_m [1 - V_f (1 + p/s)] \quad (4.45)$$

When the same external stress  $\sigma$  is applied to the short fiber composite model and to its equivalent homogeneous material model, the same strain energy is presumed for these two models. With this assumption, the longitudinal Young's modulus of the short fiber composite model  $E_L$  can be expressed as follows.

$$E_L = \frac{E_c E_m}{E_c \frac{p/s}{1 + p/s} + E_m \frac{1}{1 + p/s}} \quad (4.46)$$

By substituting the value for  $E_c$  from equation (4.45) into equation (4.46), one can get the elastic modulus,  $E_L$ , in the

longitudinal direction. The elastic-viscoelastic correspondence principle allows one to express the extensional modulus in the x-direction as a complex quantity

$$E_x^* = E_x' + iE_x'' \quad (4.47)$$

where  $E_x'$  and  $E_x''$  are the storage and loss moduli, respectively; the ratio  $\eta_x = E_x''/E_x'$  is the loss factor, and is a measure of the damping. The expression for  $E_x^*$  is obtained in terms of the longitudinal modulus  $E_L^*$ , transverse modulus  $E_T^*$ , shear modulus  $G_{LT}^*$ , and the Poisson's ratio  $\nu_{LT}$ , where the transverse and shear moduli are obtained by use of Halpin-Tsai equations and a modified rule of mixtures. Details of this analysis are available in [39].

#### IV.4 Optimum Synthesis Problem

The analysis presented in preceding sections clearly indicates the dependence of internal material damping in composites on the fiber and matrix geometry. In particular, the model based on Cox's shear lag theory allows us to write the loss factor in the following functional form.

$$\frac{E_x''}{E_x'} = \eta_x(E_f^*, E_m^*, G_m^*, p, s, d, D, \theta) \quad (4.48)$$

A parametric study can be conducted by varying each of

these variables, one at a time, to examine their influence on the damping. Such studies have been reported in the literature [40], but are susceptible to yielding sub-optimal results. In the present work, the analysis for damping is reformulated as a formal multidimensional optimization problem, with the following mathematical statement.

$$\text{Maximize } F(\bar{X}) \quad (4.49a)$$

$$\text{subject to } g_j(\bar{X}) \leq 0 \quad j=1,2,\dots,m \quad (4.49b)$$

$$X_i^l \leq X_i \leq X_i^u \quad (4.49c)$$

Here,  $F$  is the objective function, and, for the problem under consideration, it is the loss factor  $\eta_X$ ;  $g_j \leq 0$  represent the inequality constraints in the synthesis problem and  $X_i^l$  and  $X_i^u$  represent the lower and upper bounds on the design variables, respectively. The inequality and side constraints in the present problem were formulated for nominal values of lower and upper bounds on the geometric variables and are as follows.

$$1 \leq s/d \leq 1000 \quad (4.50a)$$

$$d \leq D - 0.001 \quad (4.50b)$$

$$2 \leq p/d \leq 5 \quad (4.50c)$$

$$0.05 \leq p/s \quad (4.50d)$$

$$0 \leq \theta \leq \pi/2 \quad (4.50e)$$

$$0.5 \leq V_f \leq \pi/4 \quad (\text{square packing}) \quad (4.50f)$$

$$0.5 \leq V_f \leq \pi/2\sqrt{3} \quad (\text{hexagonal packing}) \quad (4.50g)$$

Here  $V_f$  has been defined before as the volume fraction and is different for square and hexagonal packing geometry. The mass of a representative volume element can be written as

$$m = (\pi/4) \{ \rho_f s d^2 + \rho_m [ p D^2 + s (D^2 - d^2) ] \} \quad (4.51)$$

where  $\rho_f$  and  $\rho_m$  denote the specific weight of the fiber and matrix materials, respectively. In addition to the constraints given by inequalities (4.50a) to (4.50g), additional inequality constraints can also be imposed on the mass of the representative volume element and the extensional and shear stiffnesses of the composite specimen. The latter constraints allow for tailoring the damping requirement of the specimen, with additional requirements on its stiffness.

The optimization problem described above can be solved by any of the known methods of nonlinear programming. A feasible-usable search direction algorithm [44] was used in the present problem with satisfactory results.

Mathematical programming based algorithms such as the one used in the present study are often susceptible to

convergence to a local optimum. To circumvent this problem, three sets of initial variables were selected for the optimization problem and are shown in Tables 4.2 and 4.3. For isotropic glass fiber, a summary of results for the final design, with and without constraints on the extensional stiffness, are summarized in Table 4.4 and 4.5, respectively. Similar results for orthotropic graphite fiber, with constraints similar to the glass fiber, are shown in Tables 4.6 and 4.7.

Some basic conclusions can be deduced from the results obtained in this study. The results clearly indicate that similar graphical and numerical trends are obtained for both isotropic and the orthotropic fibers. The parametric variations in the damping with the loading angle and the fiber aspect ratio indicate that the latter is more critical to the damping at lower values of loading angles. Furthermore, increasing the volume fraction results in lower values of damping. This is to be expected because of a decrease in the polymer matrix material with increasing volume fraction. These figures also indicate a necessity to guard against the possibility of converging to local optimum because of the relatively flat variations of the loss factor with the loading angle.

Addition of a constraint on the extensional stiffness of the element gave similar results but with a lower value of the damping or loss factor. This is not unusual as

Table 4.2 Initial design for Glass Epoxy composite (length units are in mm).

case	d	D	p	s	$\theta$
1	0.010	0.050	0.040	0.010	25.
2	0.035	0.040	0.100	0.035	30.
3	0.072	0.080	0.300	0.072	40.

Table 4.3 Initial design for Graphite Epoxy composite (length units are in mm).

case	d	D	p	s	$\theta$
1	0.010	0.0212	0.0530	0.0100	5.
2	0.0053	0.0080	0.0116	0.0106	15.
3	0.0125	0.0135	0.0550	0.0125	20.

Table 4.4 Final design for Glass Epoxy composite specimen (length units are in mm).

Starting set		d	D	P	s	$\theta$	$V_f$	s/d	$\eta_x$
Square packing array	1	0.01	0.01001	0.020	0.0203	39.5	0.5	2.02	0.01531
	2	0.01	0.01014	0.020	0.0212	40.7	0.5	2.12	0.01530
	3	0.01	0.01001	0.020	0.0202	39.6	0.5	2.02	0.01531
Hexagonal packing array	1	0.01	0.01002	0.020	0.0202	36.4	0.5	2.02	0.01547
	2	0.01	0.01003	0.020	0.0203	35.4	0.5	2.03	0.01546
	3	0.01	0.01003	0.020	0.0203	35.4	0.5	2.03	0.01546

Table 4.5 Final design for Glass Epoxy composite specimen with constraint on tensile modulus (length units are in mm).

Starting set		d	D	P	s	$\theta$	$V_f$	s/d	$\eta_x$
Square packing array	1	0.01	0.0102	0.0209	0.0292	45.5	0.56	2.92	0.01470
	2	0.01	0.0103	0.0209	0.0289	38.5	0.55	2.89	0.01462
	3	0.01	0.0101	0.0208	0.0283	45.9	0.56	2.89	0.01470
Hexagonal packing array	1	0.01	0.0102	0.0206	0.0299	48.3	0.57	2.99	0.01468
	2	0.01	0.0101	0.0200	0.0272	43.3	0.57	2.73	0.01473
	3	0.01	0.0102	0.0204	0.0290	50.7	0.57	2.90	0.01463

Table 4.6 Final design for Graphite Epoxy composite specimen (length units are in mm).

Starting set		d	D	P	s	$\theta$	$V_f$	s/d	$\eta_x$
Square packing array	1	0.0053	0.00531	0.0106	0.0106	2.10	0.50	2.01	0.01636
	2	0.0053	0.00532	0.0106	0.0108	2.03	0.50	2.04	0.01633
	3	0.0053	0.00531	0.0106	0.0108	4.05	0.50	2.03	0.01633
Hexagonal packing array	1	0.0053	0.00532	0.0106	0.0108	2.16	0.50	2.04	0.01651
	2	0.0053	0.00532	0.0107	0.0108	10.4	0.50	2.04	0.01647
	3	0.0053	0.00532	0.0106	0.0108	6.80	0.50	2.03	0.01650

Table 4.7 Final design for Graphite Epoxy composite specimen with constraint on tensile modulus (length units are in mm).

Starting set		d	D	P	s	$\theta$	$V_f$	s/d	$\eta_x$
Square packing array	1	0.0053	0.00536	0.0106	0.0137	0.10	0.55	2.59	0.01538
	2	0.0053	0.00538	0.0106	0.0138	0.84	0.55	2.61	0.01536
	3	0.0053	0.00547	0.0106	0.0144	0.89	0.54	2.72	0.01531
Hexagonal packing array	1	0.0053	0.00545	0.0107	0.0158	0.	0.56	2.99	0.01539
	2	0.0053	0.00538	0.0108	0.0154	0.	0.57	2.91	0.01544
	3	0.0053	0.00549	0.0109	0.0161	0.97	0.56	3.03	0.01539



stiffness is governed by the fiber component and its increase results in a corresponding decrease in the matrix material, where the latter contributes towards the damping.

By comparing the numerical results for the square packing and hexagonal packing geometry, it is seen that there is no significant effect on the magnitude of the damping factor. However, the upper bound on the volume fraction of the hexagonal geometry is about 15% higher than for the square packing geometry. This allows for an increased stiffness in the specimen.

To study the optimum layout of the composite specimen based on the advanced shear lag model, the analysis equations of the previous study were replaced by equations that adequately model the new load distribution in the specimen. The new nonlinear optimization problem required a maximization of  $\eta_X$ , which is a function of the design variable vector  $V = \{E_f^*, E_m^*, G_m^*, p, s, d, D, \theta\}$ , and subject to constraints that place bounds on the mass and extensional stiffness of the composite specimen. The inequality and side constraints in the present problem that were formulated for nominal values of lower and upper bounds on the geometric variables are as follows:

$$\sigma_{fu} / 2r_y \leq s/d \leq 1000. \quad (4.52a)$$

$$d \leq D - 0.001 \quad (4.52b)$$

$$0.01 \leq p/s \quad (4.52c)$$

$$0 \leq \theta \leq \pi/2 \quad (4.52d)$$

$$0.5 \leq V_f \leq \pi/4 \quad (\text{square packing}) \quad (4.52e)$$

$$0.5 \leq V_f \leq \pi/2\sqrt{3} \quad (\text{hexagonal packing}) \quad (4.52f)$$

Here  $\sigma_{fu}$  is the ultimate strength of short fiber, and  $\tau_y$  is the matrix yield stress in shear. Constraint(4.52a) stems from requirements of a critical fiber length [56]. In this study, the  $\sigma_{fu}$  of glass fiber and graphite fiber are 3500 Mpa and 2750 Mpa, respectively. The matrix yield shear stress is 97 Mpa. The volume fraction  $V_f$  for square packing is written as

$$V_f = \pi d^2 / [4D^2 (1 + p/s)] \quad (4.53)$$

and for hexagonal packing as follows:

$$V_f = \pi d^2 / [2\sqrt{3} D^2 (1 + p/s)] \quad (4.54)$$

The mass of a representative volume element can be written as

$$m = (\pi/4) \{ \rho_f s d^2 + \rho_m [ p D^2 + s (D^2 - d^2) ] \} \quad (4.55)$$

where  $\rho_f$  and  $\rho_m$  denote the specific weight of the fiber and

matrix materials, respectively. In addition to constraints given by equation (4.52a) to (4.52f), inequality constraints can also be imposed on the mass of the representative volume element and the extensional stiffness of the composite specimen. The latter constraint allows for tailoring the damping requirement of the specimen, with added specification on its stiffness.

The optimization problem described above can be solved by any of the known methods of nonlinear programming. As in the Cox's shear-lag model, Zoutendijk's method of feasible-usable search directions [76] was used as the optimization algorithm to generate a sequence of optimum designs.

A typical optimum design with a constraint on the element mass is illustrated in Table 4.8. The final design for isotropic glass fiber with a constraint on the extensional stiffness, is summarized in Table 4.9. Similar results for orthotropic graphite fiber are shown in Table 4.10.

Variation in the optimum loss factor for prescribed extensional stiffness requirements is illustrated in Figure 4.10. This figure depicts the dependence of the loss factor on  $k$ , with three specific values of  $k$  chosen for comparison. The case  $k=0$  illustrates the Cox's shear lag analysis for a glass-epoxy composite and  $k=0.047$  and  $0.5$  correspond to an analysis based on the advanced shear-lag model for the same material. A hypothetical matrix material is represented as

Table 4.8 Optimum design for glass-epoxy composite using modified shear-lag analysis,  $(\sigma f_u / 2\tau_y) \leq s/d$  (length units - mm).

Packing	k	d	D	P	s	$\theta$	$V_f$	$s/d$	$\eta_x$
Square	0.	0.01	0.0124	0.039	0.197	49.5	0.5	19.7	0.01489
	0.047	0.01	0.0124	0.029	0.189	50.8	0.5	18.9	0.01487
Hexagonal	0.	0.01	0.0134	0.029	0.20	49.7	0.5	20.0	0.01489
	0.047	0.01	0.0134	0.029	0.196	50.4	0.5	19.6	0.01487

Table 4.9 Optimum design for glass-epoxy composite with constraint on extensile modulus obtained by using modified shear-lag analysis,  $(\sigma f_u/2\tau_y) \leq s/d$  (length units - mm).

Packing	k	d	D	P	s	$\theta$	$V_f$	$s/d$	$\eta_x$
Square	0.	0.01	0.0119	0.040	0.227	45.8	0.55	22.7	0.01455
	0.047	0.01	0.0119	0.034	0.188	51.0	0.56	18.5	0.01445
Hexagonal	0.	0.01	0.0128	0.030	0.197	45.9	0.55	19.7	0.01455
	0.047	0.01	0.0127	0.040	0.180	47.2	0.55	18.0	0.01450

Table 4.10 Optimum design for graphite-epoxy composite with constraint on extensile modulus obtained by using modified shear-lag analysis,  $(\sigma f_u/2\tau_y) \leq s/d$  (length units - mm)

Packing	k	d	D	P	s	$\theta$	$V_f$	$s/d$	$\eta_x$
Square	0.	.0053	.0054	0.037	0.096	18.0	0.55	18.	0.01493
	.015	.0053	.0054	.034	.098	19.7	0.56	18.4	0.01487
Hexagonal	0.	.0053	.0062	0.024	0.075	20.1	0.5	14.2	0.01458
	.015	.0053	.0062	0.024	0.079	20.7	0.5	14.8	0.01457

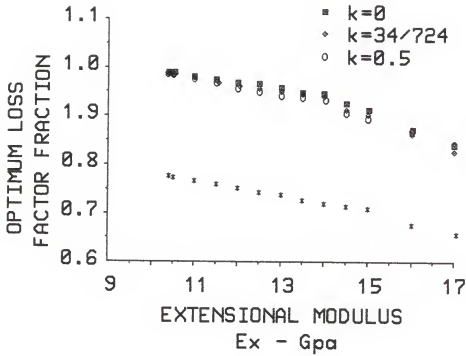


Figure 4.10 Variation of loss factor with stiffness and  $k=E_m/E_f$  (\* :  $k=0.141$ ,  $\eta_m=0.012$ ,  $\eta_{Gm}=0.014$ ).

the fourth case, with  $k=0.141$  associated with  $\eta_m=0.012$  and  $\eta_{Gm}=0.014$ . With increasing values of  $k$ , the optimum damping is lower. This is to be expected as the matrix contributes to the axial load carrying capability, generating lower interfacial shear, and hence a lower energy dissipation in the matrix material. Cox's model appears to be adequate for analysis of composites with polymer matrix materials with low extensional moduli. However, alternate shear-lag models must be explored for matrix materials with higher extensional modulus such as metal matrix composites.

## CHAPTER V

### MULTIOBJECTIVE OPTIMIZATION FOR IMPROVED STRUCTURAL DAMPING AND VIBRATION CONTROL

#### V.1 Introduction

The increased application of composite materials in structures that are subjected to dynamic loads has introduced stringent requirements on the dynamic characteristics of these materials. In addition to the requirements on stiffness and strength, a dynamic load environment also introduces the need to tailor the internal material damping characteristic. Chapter IV propose an optimum synthesis procedure for improving internal material damping by constructing a representative volume element model. The functional relationships for damping were obtained on the basis of Cox's shear-lag theory and an advanced shear-lag theory.

The enhancement of internal material damping is one approach of attaining passive control of vibration in a structural dynamics environment. The large displacements at near resonance condition can be controlled by increasing the structural damping without increasing the natural frequencies of free vibration. Another approach to reduce the resonant displacements is through an increase in the



stiffness of the structural elements. This typically results in an increase in the natural frequencies and shifts them away from resonant conditions. However, there is an attendant increase in the structural weight.

The enhancements in damping by tailoring the composite specimen as described in previous sections are limited by physical restrictions to adhere to limits on geometry variations, availability of materials, and requirements on element strength. Hence, the approach of attaching an add-on high internal damping material on a base composite structure to enhance the structural damping is both attractive and valuable. Reference [43] investigated a methodology of using add-on viscoelastic material applied on a cantilever composite beam to further improve the structural damping. Both analytical and experimental studies were performed to show that damping can be increased considerably, and maximum displacements reduced at resonant frequencies.

The present work proposes a design synthesis approach, based on the multiobjective optimization method capable of handling mixed integer, discrete and continuous design variables developed in Chapter III. This synthesis problem is clearly of a multicriterion nature, requiring a simultaneous minimization of structural weight, maximization of structural damping, and minimization of displacement at select locations on the structure. The design is subject to

constraints on the geometrical design requirements. Subsequent sections of this chapter discuss representative analytical models and their use in the design optimization study.

## V.2 Analytical Estimates of Structural Damping and Displacement for a Cantilever Beam

Consider a cantilever composite laminated beam of length  $L$ , and with a length  $a_2$  of viscoelastic layer placed as shown in Figure 5.1. The beam is clamped at the end  $x = 0$  and free at the end  $x = L$ , and is subjected to a sinusoidal excitation  $Ae^{i\Omega t}$  applied at the support. Assume the coefficient  $A$  is equal to 1 mm and the length  $L$  is equal to 125 mm. A side view of the design model which indicates the geometrical stacking sequence of plies is shown in Figure 5.2. Values of beam width  $b = 23$  mm and a thickness of the viscoelastic layer  $c = 0.38$  mm are chosen for the problem. A perfect bonding between the laminated composite and add-on viscoelastic material is assumed. The equation of motion of this design model can be written as follows

$$D^* z_{,xxxx} + \rho z_{,tt} = A e^{i\Omega t} \quad (5.1)$$

where  $D^*$  is complex flexural stiffness and can be expressed as

$$D^* = D' (1 + i\eta) \quad (5.2)$$

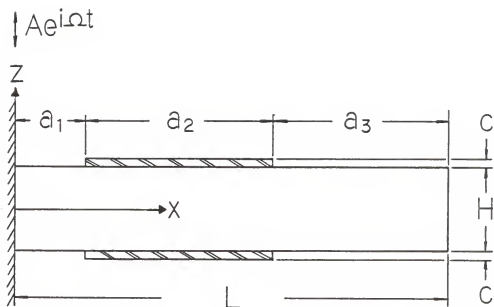


Figure 5.1 Cantilever composite beam with add-on viscoelastic layer (  $L=125$  mm,  $c=0.38$ mm ).



where  $D'$  is the real part of  $D^*$  and  $\eta$  is the loss factor or structural damping.

Since there is no simple closed-form expression to solve for the loss factor and displacements in this composite structure, a direct frequency response method [77] based on a finite element formulation was adopted for the simplicity it afforded. The beam was modeled by conventional two noded beam elements with two degrees of freedom at each node. The complex stiffness matrix and the consistent mass matrix were calculated from the element dimensions, density, and the complex flexural stiffness  $D_{11}^*$ .

The finite element model requires as an input, the flexural stiffness  $D'_{11}$ , the loss factor  $\eta$ , and the density  $\rho$  for both the bare structure and the portion containing the viscoelastic layer. Figure 5.1 shows section  $a_1$  and  $a_3$  representing bare segments, and section  $a_2$  as containing a viscoelastic layer treatment. The complex flexural stiffness of the bare portion can be expressed as the following:

$$bD_{11}^* = \frac{2}{3} t^3 \{ (\bar{Q}_{11})_{\theta 1}^* [(N_1+N_2+N_3)^3 - (N_2+N_3)^3] + (\bar{Q}_{11})_{\theta 2}^* [(N_2+N_3)^3 - N_3^3] + (\bar{Q}_{11})_{\theta 3}^* N_3^3 \} \quad (5.3)$$

where

$$(\bar{Q}_{11})_{\theta i}^* = Q_{11}^* \cos^4 \theta_i + Q_{22}^* \sin^4 \theta_i + 2(Q_{12}^* + 2Q_{66}^*) \sin^2 \theta_i \cos^2 \theta_i$$

$$i = 1, 2, 3 \quad (5.4)$$

and  $Q_{11}^*$ ,  $Q_{22}^*$ ,  $Q_{12}^*$ ,  $Q_{66}^*$  are the functions of  $E_L^*$ ,  $E_T^*$ ,  $\nu_{LT}^*$  and  $G_{LT}^*$ . These expressions were largely obtained from [56].

For a continuous fiber composite, the longitudinal modulus  $E_L^*$  can be expressed by the rule of mixtures

$$E_L^* = E_f^* V_f + E_m^* V_m \quad (5.5)$$

where

$$E_f^* = E_f' + (1 + i\eta_f) \quad (5.6)$$

$$E_m^* = E_m' + (1 + i\eta_m) \quad (5.7)$$

Similarly,  $\nu_{LT}^*$ ,  $E_T^*$  and  $G_{LT}^*$  can also be expressed by invoking the rule of mixtures. For a discontinuous fiber composite, the complex longitudinal modulus can be derived from a representative volume element of an aligned short fiber model (Chapter IV) and be expressed as follows.

$$E_L^* = \frac{E_c^* E_m^*}{E_c^* \frac{p/s}{1 + p/s} + E_m^* \frac{1}{1 + p/s}} \quad (5.8)$$

where

$$E_C^* = E_f^* V_f (1 + p/s) \left[ 1 - \frac{\tanh(\beta^* s/2)}{\beta^* s/2} \right] + E_m^* [1 - V_f (1 + p/s)] \quad (5.9)$$

The volume fraction of fiber  $V_f$  and parameter  $\beta^*s$  are dependent on the fiber packing arrangement in the matrix material. These and other related formulations can be found in chapter IV.

The complex stiffness  $bD_{11}^*$  can be further separated into a real part  $bD'_{11}$  and an imaginary part  $bD''_{11}$  by applying the elastic-viscoelastic correspondence principle. The damping value of the bare section for this laminated beam  $b\eta$  is thus the ratio of the imaginary and real parts as follows.

$$b\eta = bD''_{11} / bD'_{11} \quad (5.10)$$

The density of the bare part of composite beam  $b\rho$  can be expressed simply from the rule of mixtures

$$b\rho = V_f \rho_f + (1 - V_f) \rho_m \quad (5.11)$$

where  $\rho_f$  and  $\rho_m$  are the density of the fiber and matrix materials, respectively.

The complex flexural stiffness of the section which is covered with viscoelastic material on the top and bottom

surface can be written as follows

$$\nu D_{11}^* = b D_{11}^* + \frac{2}{3} (\bar{Q}_{11})_{vis} \{ [(N_1 + N_2 + N_3)t + c]^3 - (N_1 + N_2 + N_3)^3 t^3 \} \quad (5.12)$$

where  $(\bar{Q}_{11})_{vis}$  of the viscoelastic layer material can be obtained from experimental observations. In this manner, the loss factor of viscoelastic material  $\eta_{vis}$  can be calculated as well. In the present study, values of  $(Q_{11})_{vis}$  and  $\eta_{vis}$  are assumed to be 11.0 Gpa and 0.52, respectively. Once again, using the elastic-viscoelastic correspondence principal to separate  $\nu D_{11}^*$  into real part  $\nu D_{11}'$ , and imaginary part  $\nu D_{11}''$ , the damping of add-on material section  $\nu\eta$  can be represented as follows.

$$\nu\eta = \nu D_{11}'' / \nu D_{11}' \quad (5.13)$$

The density of add-on viscoelastic section can be written as

$$\nu\rho = V_V \rho_V + (1 - V_V) b\rho \quad (5.14)$$

where  $V_V$  is the volume fraction of add-on viscoelastic material and  $\rho_V$  is the density of this material and is assumed to be equal to  $\rho_m$  in this study.

The computations of  $b D_{11}'$ ,  $\nu D_{11}'$ ,  $b\eta$ ,  $\nu\eta$ ,  $b\rho$  and  $\nu\rho$  are important in the finite element formulation [77], where the



response of the structure is determined for a forcing function at a given frequency. The computations are repeated over a range of frequencies to generate the frequency response characteristics from which the resonant frequency and damping can be calculated.

The structural damping corresponding to the first node can be computed by using the formulation of reference [78]. and is expressed as follows

$$\eta = 1.56599 \ z(0)/ z(L) \quad (5.15)$$

where  $z(0)$  and  $z(L)$  are the wall (or root) and tip amplitudes, respectively. The material constants used in this study are listed in Table 2.1 of Chapter II.

### V.3 Formulation of Multiobjective Optimum Design With Mixed Design Variables

The optimal design problem under study is characterized by the existence of three criteria. The displacement  $z$  at the tip must be minimized with a minimum total weight and maximization of structural damping. The design of this laminated composite beam depends upon the material properties, add-on material, and on the geometry and configuration variables such as lamina thickness, number of plies, fiber orientation in each ply, and the volume

fraction. These variables are of both the continuous and discrete type. With reference to Figure 5.2, the depth of the beam can be described by three layers, with each layer containing  $N_1$ ,  $N_2$ , and  $N_3$  plies of thickness  $t$ . The fiber orientations in these layers are given by  $\theta_1$ ,  $\theta_2$ , and  $\theta_3$ , respectively. The length of add-on material variables is given by  $a_2$  and the distances to the root and tip are  $a_1$  and  $a_3$ , respectively. The optimization problem is formulated as a multidimensional nonlinear programming problem with continuous, discrete and integer variables. The mathematical problem statement is as follows.

$$\text{Minimize } (W_T, -\eta, A_p) \quad (5.16a)$$

where

$$W_T = L \{ b\rho [bH(a_1+a_3) + v\rho ba_2(H+2c)] \} \quad (5.16b)$$

$$\eta = 1.56599 \ z(0) / z(L) \quad (5.16c)$$

$$A_p = z(L) \quad (5.16d)$$

subject to inequality and equality constraints,

$$H \geq 3.5 \text{ mm} \quad (5.17a)$$

$$H \leq 10.0 \text{ mm} \quad (5.17b)$$

$$a_1 + a_2 + a_3 = L \quad (5.17c)$$

where  $W_T$  is the total structural weight,  $\eta$  is the structural damping, and  $z(L)$  is the tip amplitude obtained as a result of the loading condition defined in Figure 5.1. The thickness of each ply was considered to be a discrete variable, with admissible values selected from the following set.

$$t = (0.1, 0.125, 0.15, 0.175, 0.225, 0.275, 0.325, 0.375)$$

The numbers of plies in each of the three layers were considered as integer variables and allowed to assume values between 3 and 50. The fiber orientation were allowed to vary between  $-90$  and  $+90$  degrees and the volume fraction bounded between 0.5 and 0.9. The locational variables of the viscoelastic layer  $a_1$ ,  $a_3$ , and  $a_2$  were allowed to vary between 0 and  $L$ . The fiber orientation  $\theta$ , volume fraction  $V_f$ , and length parameters  $a_1$ ,  $a_2$  and  $a_3$  are variables of the continuous type. An adaptive finite element nodes generation technique was used in this problem to accommodate the variation of  $a_1$ ,  $a_2$  and  $a_3$ . For the optimization problem described above, the initial design was selected as follows.

$$\begin{array}{llll}
 t = 0.25 \text{ mm} & N_1 = 8 & N_2 = 8 & N_3 = 8 \\
 \theta_1 = 10^\circ & \theta_2 = 40^\circ & \theta_3 = -40^\circ & V_f = 0.6 \\
 a_1 = 0.2L & a_2 = 0.7L & a_3 = 0.1L & 
 \end{array}$$

#### V.4 Multiobjective Optimum Design for Dynamically Responding Composite Structure

The numerical results for the multiobjective optimum design involving damping due to an add-on viscoelastic layer on a base structure, is presented in this section. Initially, a systematic study was conducted to determine the influence of the viscoelastic layer on the resonant frequency, the structural damping and the tip displacement under a given dynamic loading. Two sets of design data were used in this preliminary work. The first set corresponded to a low material damping and high stiffness characteristics, and the second to a higher material damping and lower stiffness. Figures 5.3 to 5.8 summarize results of this parametric study for the first set. Figure 5.3 to 5.5 show the relationship between the structural damping and first natural frequency, and add-on material length. Figure 5.6 to 5.8 show the variation of amplitude with the add-on material length.

Some pertinent observations can be drawn from the foregoing results. Both set of designs show that a decreasing resonant frequency is obtained with increasing distance  $a_1$ . Both the damping and resonant frequency

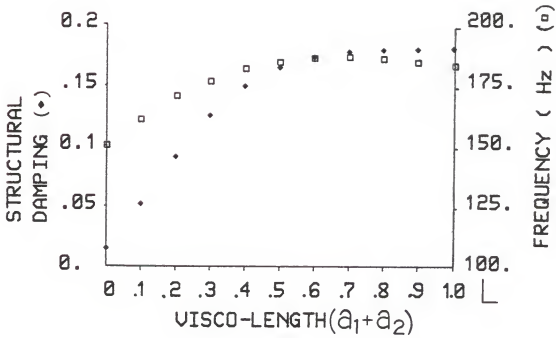


Figure 5.3 The variations of structural damping and first natural frequency with different length of add-on material  $a_2$  ( $a_1 = 0$ ).

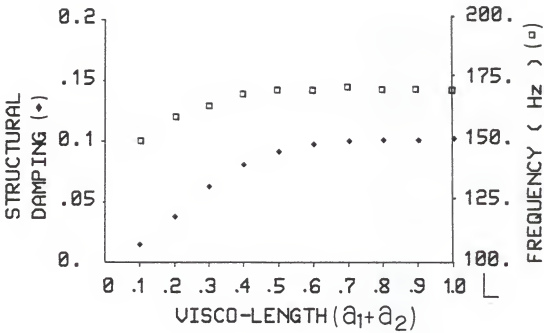


Figure 5.4 The variations of structural damping and first natural frequency with different length of addition material  $a_2$  ( $a_1 = 0.1L$ ).

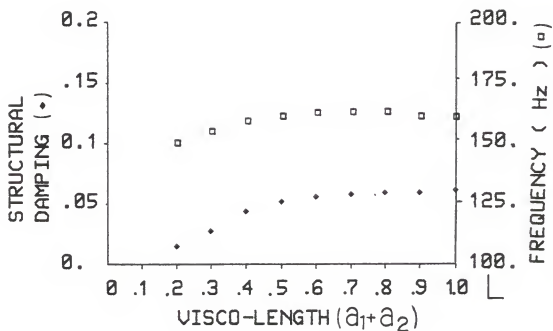


Figure 5.5 The variations of structural damping and first natural frequency with different length of add-on material  $a_2$  ( $a_1 = 0.2L$ ).

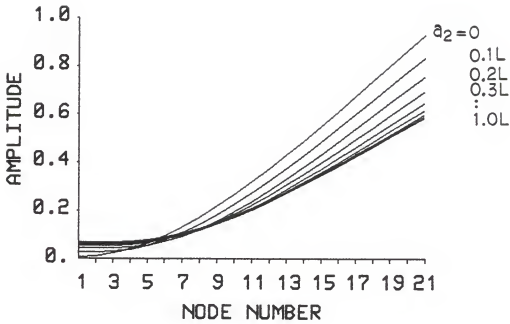


Figure 5.6 The variation of structural amplitude shape with different length of add-on material  $a_2$  ( $a_1 = 0$ ).



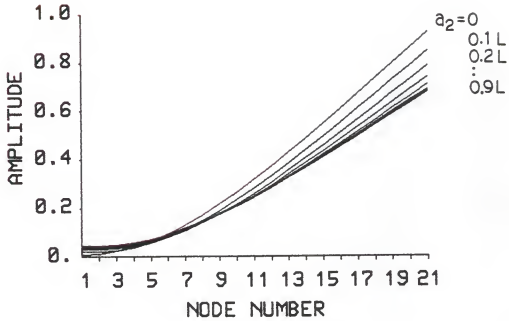


Figure 5.7 The variation of structural amplitude shape with different length of add-on material  $a_2$  ( $a_1=0.1L$ ).

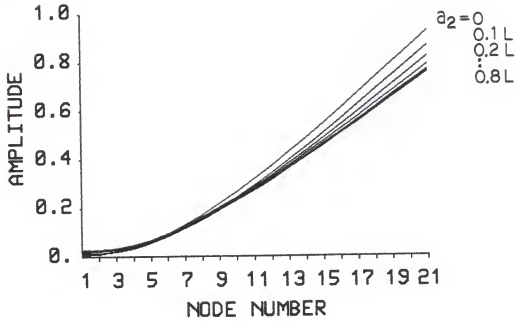


Figure 5.8 The variation of structural amplitude shape with different length of add-on material  $a_2$  ( $a_1 = 0.2L$ ).

increase with  $a_2$  until about  $a_2 = 0.6L$ . After that, the damping keeps on increasing while the resonant frequency shows a decrease. Resonant frequency is influenced both by the location and length of add-on viscoelastic material, as well as the internal material damping. This study also shows that the highest structural damping value always occurs in a situation where the composite beam is fully covered by a viscoelastic material layer. The structural damping value drops very sharply when the add-on material is placed in a manner that its starting point is away from the root. From the standpoint of dynamic amplitude,  $a_1$  and  $a_2$  are also significant. In the case where  $a_1$  is zero, the amplitude decreases as  $a_2$  is increased. However, there is a very slight influence in the amplitude when  $a_2$  is larger than about  $0.7L$ . When  $a_1$  is not zero, the amplitude values approach those corresponding to the bare structure as  $a_1$  is increased. In other words, the effect of add-on material is gradually diminished. The numerical results for the amplitude show that the minimum tip displacement occurs when  $a_2$  is around  $0.8L$  and the add-on layer starts from the wall. The above observation indicates the need to look at the overall optimization problem as obtaining the optimum values of  $a_1$ ,  $a_2$  and  $a_3$ , as well as optimum designs of laminated composite structures.

The continuous optimization problems in the present work were very highly nonlinear, but were linearized by

approximating the objective function and constraints by a first order Taylor series representation. An optimum value of each candidate criterion was first obtained by considering them individually and treating all design variables as continuous. These results are present in Table 5.1 which shows significant differences in optimum design variables for the individual objective function optimizations. For instance, in comparing the design for minimum weight and tip displacement with that for maximum damping, the latter shows an upper bound of volume fraction, upper bound of structural height, vanishing  $a_1$ , and  $a_2=0.7L$ . Maximizing the damping results in significant differences of loading angle and stacking sequences, and results in a lower bound of volume fraction, a full length application of the viscoelastic layer on the structure, and an optimum damping value 0.4118. This value is close the damping value of 0.52 for the viscoelastic material. Minimizing the tip amplitude results in the highest value of stiffness and natural frequency  $\omega_1$ .

The ratio of the tip displacement for the bare structure and one fully covered with the add-on material is 5.54 for maximum damping, and 1.1 for minimum tip amplitude. This indicates that maximizing the structural damping tends to reduce the resonant displacement. The natural frequency obtained when maximizing the structural damping is lower than the value obtained when increasing structural

Table 5.1 Optimum continuous design for individual objective criterion.

Objective Criteria $W_T$ = weight $\eta$ = damping $A_p$ = tip amplitude	t (mm)	$N_1$	$N_2$	$N_3$	$\theta_1$	$\theta_2$	$\theta_3$	$V_f$	$a_1$	$a_2$	$a_3$	$\omega_1$ (Hz)
Minimum weight $W_T = 0.1858 \text{ N}$ $\eta = 0.013$ $A_p = 8.02 \text{ mm}$	0.1	5.78	5.78	5.78	10.	40.	-40.	0.5	0.6	0.	0.4	49.3
Maximum damping $\eta = 0.4118$ $W_T = 0.1873 \text{ N}$ $A_p = 8.54 \text{ mm}$	0.1	3.02	4.25	10.2	-9.28	3.75	5.11	0.5	0.	1.	0.	84.4
Minimum amplitude $A_p = 0.06008 \text{ mm}$ $W_T = 0.7115 \text{ N}$ $\eta = 0.0166$	0.194	19.7	3.	3.	-2.4	31.	-40.	0.9	0.	0.71	0.29	585.7

stiffness.

Table 5.2 summarizes optimum designs arrived at by using the multiobjective design strategy for mixed variables described in an earlier section, and for a choice of two sets of weighting coefficients. A choice of weighting coefficients of (0.333, 0.333, 0.333), represents the case where each of the objective criteria are equally important. Another set of weighting coefficients of (0.25, 0.45, 0.30) represents a different relative rank of the objective criteria. For both of these cases, the optimum starting location of the viscoelastic layer was at the wall. There are, however, differences in the optimum values of other variables such as lamina ply thickness  $t$ , and the stacking sequences.

Table 5.2 Optimum designs for different weighting coefficients.

Optimize Objective criteria $W_T$ = weight $\eta$ = damping $A_p$ = tip amplitude	Weighting Coefficients ( $W_T, \eta, A_p$ )	$t$ (mm)	$N_1$	$N_2$	$N_3$	$\theta_1$	$\theta_2$	$\theta_3$	$V_f$	$a_1$	$a_2$	$a_3$	$\omega_1$ (Hz)
$W_T = 0.4826 \text{ N}$ $\eta = 0.03607$ $A_p = 0.1570 \text{ mm}$	(0.33, 0.33, 0.33)	0.225	12	3	4	-2.6	2.74	-56.1	0.51	0	0.79	0.21	442.45
$W_T = 0.4922 \text{ N}$ $\eta = 0.03691$ $A_p = 0.1485 \text{ mm}$	(0.25, 0.45, 0.30)	0.275	10	3	3	-3.5	7.34	-55.6	0.50	0	0.81	0.19	448.82

## CHAPTER VI

### CONCLUDING REMARKS

The continuous optimization problems encountered in the present study involving composite materials were highly nonlinear. A piecewise linearization of these problems was implemented by approximating the objective functions and constraints by a first order Taylor series representation. Initially, a 25% move limit on the design variables was adopted and found to contribute to instability in the convergence behavior. Consequently, a tighter move limit on design variable change ( $\pm 10\%$ ) was imposed in all solutions. Although the tight move limit improves the convergence pattern, it results in higher computational costs. As is typical of all gradient based methods, the solutions are, at best locally optimum in a nonconvex design space. Several starting designs were therefore used to determine the best solutions.

Since symmetrically laminated fiber composites are widely used in practical applications, the numerical problems in this study were largely restricted to this configurations. However, a similar approach with some modifications in analysis is applicable for unsymmetrical laminated composites. The numerical results presented in



this work that relate to fiber reinforced composites were obtained on the basis of the following additional assumptions:

1. The matrix epoxy behaves as a linear, isotropic, viscoelastic material.
2. All fibers behave as linear viscoelastic materials.
3. The dependence of modulus on frequency is not included in the present analysis.

The friction loss is independent of the frequency when the frequency of cyclical stress is below 50 Hz and strain is below the elastic limit. This was examined in the experimental work of eighteen different solids by Kimball and Lovell [34].

## VI.1 Conclusions

This research describes the development and implementation of an optimization strategy for problems which include a mixture of continuous, discrete and integer design variables. A modified branch and bound approach was used in this development. The principal advantages of the present algorithm include the ability to predict the maximum storage requirements, an efficient fathoming procedure, and a clear record of the optimization process that can be used for additional studies.

The modified branch and bound approach is used to solve structural design problems that are described in terms of

continuous and discrete variables. In particular, a minimum weight design of a laminated composite beam structure for constraints on displacements, frequencies, and strength requirements was chosen, and this included all characteristics of the mixed variable problem. The results obtained in these numerical experiments supported the applicability of the method.

This work further presents a methodology for solving multiobjective optimization problems that involve a mix of discrete, continuous, and integer design variables. The method combines a discrete variable variant of the global criterion approach with a modified branch and bound strategy. The mathematical basis of the selection of ideal solutions for this approach is also presented. For discrete and integer design variable problems, it is shown that the ideal solution required in the global criterion strategy is one that corresponds to a continuous optimal solution. This study has also attempted to establish the advantages of a multicriterion optimization strategy in relation to the conventional approach of using a scalar objective function, and accounting for other competing criteria by design constraints. The method developed in this work was implemented on illustrative multiobjective design problems with encouraging results.

This research also presents an approach in which a formal optimization strategy is used to study the internal

material damping characteristics of short-fiber, polymer matrix composites. The use of such techniques is shown to yield useful information in tailoring composite materials for damping and stiffness characteristics. Two distinct models for predicting internal material damping are used in the analysis. For polymer matrix composites, the differences in the numerical values of the optimal damping from these models are not significant, and this is attributed to the low tensile modulus for the matrix material. Therefore, the commonly used Cox's shear lag model appears to be adequate for analysis of composite with polymer matrix materials with low extensional moduli. However, alternate advanced shear lag models must be explored for matrix materials with higher extensional moduli as in metal matrix composites.

This report also examines the optimum synthesis of laminated composite structures with an add-on viscoelastic material layer to improve structural damping. Such an optimization is performed in conjunction with the internal material damping using either Cox's or an advanced shear lag theory. For the solution to the problem involving dynamic loads, the multiobjective optimization strategy in a mixed design variable space is used effectively to accommodate multiple criteria including structural weight, damping and dynamic displacement amplitude.

## VI.2 Recommendations for Future Work

The computational resource requirements for the design optimization problems described herein were somewhat demanding. The solution time increased with the number of integer/discrete variables, the number of design constraints and the complexities modeled in the finite element program. Further effort needs to be expended in reducing these computational requirements. The scope of such a study may include improvement in the storage scheme, and increased efficiency of a programming algorithm. In the present form, a physically meaningful solution really requires the capabilities of a supercomputer. Further research is also necessary into exploring alternative search algorithms that are not as susceptible to convergence to a local optimum.

The work pertaining to improving the internal material damping in chopped-fiber reinforced composites should be extended to include the shape of the fiber ends as design variables in the synthesis problem. Inclusion of random fiber orientations, and modeling imperfections in fiber-matrix bonding, including their influence on damping, is another area of possible research.

This research report proposes a theoretical approach for reducing dynamic displacement amplitudes by introducing passive damping of add-on viscoelastic materials. The problem involves a multiobjective optimization in a space of

continuous, integer and discrete design variables. The present work assumes a perfect bonding between the viscoelastic layer and the base structure. In actuality, the add-on viscoelastic material available commercially [79] consists of a layer of viscoelastic damping material and a constraining layer. The viscoelastic material is constrained with the constraining layer with rigidity comparable to that of the composite beam. The viscoelastic material is therefore forced to deform in shear and will dissipate considerable energy through shear deformation. A revised analytical and numerical model which accounts for this phenomenon must be developed to integrate into the present sizing procedure. In such an extension, the thickness of viscoelastic material can be chosen as an additional discrete design variable. Finally, additional effort is required in obtaining the optimum viscoelastic material application for higher modal response. It is expected that for these higher modes, a discontinuous material application along the base structure may be more effective.

## REFERENCES

1. Lazan, B.J., "Damping Properties of Materials and Material Composites," Applied Mechanics Review, 15(2), pp. 81-88, 1962.
2. Salama, M., Hamidi, M., and Demsetz, L., "Optimization of Controlled Structures," Paper presented at the JPL Workshop on Identification and Control of Flexible Space Structures, San Diego, CA, June, 1984.
3. Khot, N.S., Eastep, F.E., and Venkayya, V.B., "Optimal Structural Modification to Enhance the Optimal Active Vibration Control of Large Flexible Structures," AIAA paper 85-0627, Presented at the AIAA/ASME/ASCE/AHS 26th Structures, Structural Dynamics and Materials Conference, Orlando, FL, April 1985.
4. Schmit, L. A., Jr., "Structural Design by Systematic Synthesis," Proceedings of 2nd Conference on Electronic Computation, ASCE, New York, pp. 105-122, 1960.
5. Berke, L., and Khot, N. S., "Use of Optimality Criteria Methods for Large Scale Systems," AGARD LS No. 70, Structural Optimization, pp. 1-29, October, 1974.
6. Levy, R., and Parzynski, W., "Optimality Criteria Solution Strategies in Multiple Constraint Design Optimization," 22nd Structures, Structural Dynamics and Materials Conference, Atlanta, Georgia, April 6-8, 1981.
7. Khan, M. R., "Optimality Criterion Techniques Applied to Frames Having Nonlinear Cross Sectional Properties," 22nd Structures, Structural Dynamics and Materials Conference, Atlanta, Georgia, April 6-8, 1981.
8. Levy, R., "Optimality Criteria Design and Stress Constraint Processing," 11th ONR Naval Structural Mechanics Symposium, Optimum Structural Design, Tucson, Arizona, October 19-22, 1981.
9. Walsh, G.R., Methods of Optimization, John Wiley and Sons, New York, 1977.

10. Fabozzi, E.J., and Valente, J., "Mathematical Programming in American Companies: A Sample Survey," Interfaces, 7(1), pp. 93-98, November, 1976.
11. Hartley, R., Linear and Nonlinear Programming: An Introduction to Linear Methods in Mathematical Programming. Halsted Press, New York, 1985.
12. Schrijver, A., Theory of Linear and Integer Programming, John Wiley and Sons, New York, 1986.
13. Bazarra, M.S., and Shetty, C.M., Nonlinear Programming: Theory and Algorithm, John Wiley and Sons, New York, 1979.
14. Reklaitis, G.V., Ravindran, A., and Ragsdell, K.M., Engineering Optimization: Methods and Applications, John Wiley and Sons, New York, 1983.
15. Balinski, M.L., "Integer Programming: Methods, Uses, Computations," Management Science, 12(3), pp. 253-313, November, 1965.
16. Beale, E.M.L., "Survey of Integer Programming," Operational Research Quarterly, 16(2), pp. 219-228, 1965.
17. Benichou, M., Gauthier, J.M., Girodet, P., Hentges, B., Ribiere, G., and Vincent, O., "Experiments in Mixed-Integer Linear Programming," Mathematical Programming, 1(1), pp. 76-94, October, 1971.
18. Forrest, J.J.H., Hirst, J.P.H., and Tomlin, J.A., "Practical Solution of Large Mixed Integer Programming Problems with UMPIRE," Management Science, 20(5), pp. 736-773, January, 1974.
19. Geoffrion, A.M., and Marsten, R.E., "Integer Programming Algorithm: A Framework and State-of-the Art Survey," Management Science, 18, pp. 465-491, 1972.
20. Mitra, G., "Investigation of Some Branch and Bound Strategies for the Solution of Mixed Integer Linear Program," Mathematical Programming, 4(2), pp. 155-170, April, 1973.
21. Kaufmann, A., and Henry-Labord'ere, A., Integer and Mixed Programming, Academic Press, New York, 1977.
22. Garfinkel, R.S., and Nemhauser, G.L., Integer Programming, John Wiley and Sons, New York, 1972.

23. Gupta, O.K., and Ravindran, A., "Nonlinear Integer Programming and Discrete Optimization," Trans. of the ASME, 105, pp. 160-164, June, 1983.
24. Pareto, V., Cours D'economie Politique, F.Rouge, Lausanne. 1896.
25. Cohon, J.L., Multiobjective Programming and Planning, Academic Press, New York, 1978.
26. Hwang, C.L., and Masud, A.S.M., Multiple Objective Decision Making: Methods and Applications; A State-of-Art Survey, Springer-Verlag, Lecture Notes in Economics and Mathematical Systems, Vol.164, Berlin-Heidelberg-New York, 1979.
27. Zeleny, M., Multiple Criteria Decision Making, McGraw-Hill, New York, 1981.
28. Goicoechea, A., Hensen, D., and Duckstein, L., Multiobjective Decision Analysis with Engineering and Business Applications, John Wiley and Sons, New York, 1982.
29. Koski, J., "Multicriterion Optimization in Structural Design," Proceedings of the International Symposium on Optimum Structural Design, 11th ONR Naval Structural Mechanics Symposium, Tucson, Arizona, October, 19-22, 1981.
30. Sawaragi, Y., Nakayama, H., and Tanino, T., Theory of Multiobjective Optimization, Academic Press, New York, 1985.
31. Tauchert, T.R., and Adibhatla, S., "Optimum Elastic Design of a Reinforced Beam," Journal of Composite Materials, 16, pp. 433-445, September, 1982.
32. Bauchau, O.A., "Optimal Design of High Speed Rotating Graphite/Epoxy Shafts," Journal of Composite Materials, 17, pp. 170-181, March, 1983.
33. Liao, D.X., Sung, C.K., and Thompson, B.S., "The Optimal Design of Symmetric Laminated Beams Considering Damping," Journal of Composite Materials, 20, pp. 485-501, September, 1986.
34. Kimball, A.L., and Lovell, D.E., "Internal Friction in Solids," Physical Review, 30, pp. 948-959, December, 1927.



35. Crandall, S.H., "The Role of Damping in Vibration Theory," Journal of Sound and Vibration, 11(1), pp. 3-18, 1970.
36. Suarez, S.A., Gibson, R.F., and Deobald, L.R., "Development of Experimental Technique for Measurement of Damping in Composite Materials", 1983 Fall meeting Proceedings, Society for Experimental Stress Analysis, Salt Lake City, Utah, pp. 55-60, November, 1983.
37. Gibson, R.F., Chaturvedi, S.K., and Sun, C.T., "Complex Moduli of Aligned Discontinuous Fiber-Reinforced Polymer Composites", Journal of Material Science, 17, pp. 3499-3509, 1982.
38. Gibson, R.F., and Yau, A., "Complex Moduli of Chopped Fiber and Continuous Fiber Composites: Comparison of Measurement with Estimated Bounds," Journal of Composite Materials, 14, pp. 155-167, 1980.
39. Sun, C.T., Chaturvedi, S.K., and Gibson, R.F., "Internal Damping of Short-Fiber Reinforced Polymer Matrix Composites," Computers and Structures, 20(1-3), pp. 391-400, 1985.
40. Sun, C.T., Gibson, R.F., and Chaturvedi, S.K., "Internal Material Damping of Polymer Matrix Composite Under Off-Axis Loading," Journal of Material Science, 20, pp. 2575-2585, 1985.
41. Plunkett, R., and Lee, C.T., "Length Optimization for Constrained Viscoelastic Layer Damping," Journal of Acoustical Society of America, 48, pp. 150-161, 1970.
42. Nashif, A.D., Jones, D.I.G., and Henderson, J.P., Vibration Damping, John Wiley and Sons, New York, 1985.
43. Sun, C.T., Sankar, B.V., Bouadi, H., and Hu, S., "Improvement in Damping by Using Viscoelastic Layer on Laminated Composite Material," ASME Winter Annual Meeting, Boston, Massachusetts, December 13-18, 1987.
44. Glover, F., and Sommer, D., "Pitfalls of Rounding in Discrete Management Decision Variables," Decision Sciences, 22(4), pp. 445-460, December, 1975.
45. Gomory, R.E., "An Algorithm for Integer Solutions to Linear Programs," Princeton-IBM Mathematics Research Project, Technical Report 1, November, 1958.

46. Land, A.H., and Doig, A.G., "An Automatic Method of Solving Discrete Programming Problems," Econometrics, 28, pp. 497-520, 1960.
47. Dakin, R.J., "A Tree-Search Algorithm for Mixed Integer Programming Problems," Computer Journal, 8(3), pp. 250-255, 1965.
48. Little, J.D.C., Murty, K.G., Sweeney, D.W., and Karel, C., "An Algorithm for the Travelling Salesman Problem," Operations Research, 11, pp. 972-989, 1963.
49. Beightler, C.S., Phillips, D.T., and Wilde, D.J., Foundations of Optimization, pp. 154-160, Prentice-Hall Inc., Englewood, Cliffs, 1979.
50. Vanderplaats, G. N., "An Efficient Feasible Direction Algorithm for Design Synthesis," AIAA Journal, 22(11), pp. 1633-1640, October, 1984.
51. Vanderplaats, G. N., Numerical Optimization Techniques for Engineering Design, McGraw-Hill, New York, 1984.
52. Zangwill, W.I., Nonlinear Programming: A Unified Approach, Prentice-Hall, Englewood, Cliffs, N.J., 1969.
53. Morris, A.J. ed., Foundations of Structural Optimization: A Unified Approach, John Wiley and Sons, New York, 1982.
54. Ragsdell, K.M., and Phillips, D.T., "Optimal Design of a Class of Welded Structures Using Geometric Programming," ASME Journal of Engineering for Industry, 98(3), pp. 1021-1025, August, 1976.
55. Whitney, J.M., Browning, C.E., and Mair, A., "Analysis of the Flexure Test for Laminated Composite Materials," Composite Materials: Testing and Design (Third Conference), ASTM STP 546, pp. 30-45, 1974.
56. Agarwal, B.D., and Broutman, L.J., Analysis and Performance of Fiber Composites, John Wiley and Sons, Inc., New York, 1980.
57. Whitney, J.M., Structural Analysis of Laminated Anisotropic Plates, Technomic Publishing Co. Inc., Lancaster, Pa., 1987.
58. Jones, R.M., Mechanics of Composite Materials, Script Book Co., Washington, D.C., 1975.

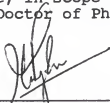
59. Baier, H., "Über Algorithmen zur Ermittlung und Charakterisierung Pareto-optimaler Lösungen bei Entwurfsaufgaben elastischer Tragwerke," ZAMM, 57, pp. 318-320, 1977.
60. Baier, H., "Mathematische Programmierung zur Optimierung von Tragwerken Insbesondere bei Mehrfachen Zielen," Ph.D. Thesis, Darmstadt University, D17, 1978.
61. Koski, J., "Truss Optimization with Vector Criterion," Tampere University of Technology, Publications 6, Tampere, 1979.
62. Osyczka, A., "An Approach to Multicriterion Optimization Problems for Engineering Design," Comp. Meths. Appl. Mech. Eng. 15, pp. 309-333, 1978.
63. Osyczka, A., "An Approach to Multicriterion Optimization for Structural Design," Proceedings of the International Symposium on Optimum Structural Design, 11th ONR Naval Structural Mechanics Symposium, Tucson, Arizona, October 19-22, 1981.
64. Rao, S.S., and Hati, S.K., "Game Theory Approach in Multicriteria Optimization of Function Generating Mechanisms," J. Mech. Des. Trans. ASME, 101, pp. 398-405, 1979.
65. Leitmann, G., "Some Problems of Scaler and Vector-Valued Optimization in Linear Viscoelasticity," Journal of Optimization Theory and Applications, 23, pp. 93-99, 1977.
66. Boychuk, L.M., and Ovchinnikov, V.O., "Principal Methods for Solution of Multi-Criteria Optimization Problems (survey)," Soviet Automatic Control, 6(3), pp. 1-4, 1973.
67. Salukvadze, M.E., "On the Existence of Solutions in Problems of Optimization Under Vector Valued Criteria," Journal of Optimization Theory and Applications, 13(2), pp. 430-468, 1974.
68. Bert, C.W., and Clary, R.R., "Evaluation of Experimental Methods for Determining Dynamic Stiffness and Damping of Composite Materials," Testing and Design (3rd Conference), ASTM STP 543, Philadelphia, 1974.
69. Nelson, D.J., and Hancock, J.W., "Interfacial Slip and Damping in Fiber Reinforced Composites," Journal of Material Sciences, 13, pp. 2429-2440, 1978.

70. Gibson, R.F., and Plunkett, R., "Dynamical Mechanical Behavior of Fiber Reinforced Composites: Measurement and Analysis," Journal of Composite Materials, 10, pp. 325-341, 1976.
71. Bert, C.W., "Composite Materials: A Survey of the Damping Capacity of Fiber Reinforced Composites," Damping Applications for Vibration Control, ASME AMD-38, pp. 53-63, 1980.
72. Mclean, D., and Read, B.W., "Storage and Loss Moduli in Discontinuous Composites," Journal of Material Sciences, 10, pp. 481-492, 1975.
73. Sun, C.T., and Wu, J.K., "Stress Distribution of Aligned Short-Fiber Composites Under Axial Load," Journal of Reinforced Plastics and Composites, 3, pp. 130-144, 1984.
74. Cox, H.L., "The Elasticity and Strength of Paper and Other Fibrous Materials," British Journal of Applied Physics, 3, pp. 72-79, 1952.
75. Fukuda, H., and Chou, T.W., "An Advanced Shear-Lag Model Applicable to Discontinuous Fiber Composites," Journal of Composite Materials, 15, pp. 79-91, 1981.
76. Rao, S.S., Optimization--Theory and Applications, Wiley Eastern Limited, New York, 1979.
77. Johnson, C.D., and Kienholz, D.A., Austin, E.M., and Schneider, M.E., "Finite Element Design of Viscoelastically Damped Structures," Vibration Damping 1984 Work Shop Proceedings, AFWAL-TR-84-3064, Editor: Lynn Rogers, Wright-Patterson Air Force Base, Ohio 45433, pp. HH1-HH27, November, 1984.
78. Gibson, R.F., Yau, A., and Riegner, D.A., "An Improved Forced Vibration Technique for Measurement of Material Damping," Experiment Techniques, 6(2), pp. 10-14, April, 1982.
79. Manufactured by Structural Products Department, 3M Center, St. Paul, Minnesota 55144. Contact: Mr. R. A. Frigstad, Manager of the Department.

#### BIOGRAPHICAL SKETCH

Chien-Jong Shih was born in February 1951, in Taiwan, R.O.C. In July, 1971, he received a diploma in mechanical engineering from the Min-Chi Institute of Technology. After release from obligatory military service, he was hired by Nan Ya Company of Formosa Groups as a mechanical engineer, where he worked for three years. In June 1978, he received a B.S. in Mechanical Engineering at National Taiwan Institute of Technology. He then rejoined Nan Ya Company in the capacity of chief engineer of Engineering and Design and was charged to oversee machine design and development. In August 1983, he joined the University of Florida, where he earned his M.S. in engineering mechanics in August 1985. He received his Ph.D. from the Department of Aerospace Engineering, Mechanics and Engineering Science in May 1989.

I certify that I have read this study and that in my opinion it conforms to acceptable standards of scholarly presentation and is fully adequate, in scope and quality, as a dissertation for the degree of Doctor of Philosophy.



---

Prabhat Hajela, Chairman  
Associate Professor of Aerospace  
Engineering, Mechanics and  
Engineering Science

I certify that I have read this study and that in my opinion it conforms to acceptable standards of scholarly presentation and is fully adequate, in scope and quality, as a dissertation for the degree of Doctor of Philosophy.



---

Lawrence E. Malvern  
Professor of Aerospace Engineering,  
Mechanics and Engineering Science

I certify that I have read this study and that in my opinion it conforms to acceptable standards of scholarly presentation and is fully adequate, in scope and quality, as a dissertation for the degree of Doctor of Philosophy.



---

Chang-Tsan Sun  
Professor of Aerospace Engineering,  
Mechanics and Engineering Science

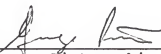
I certify that I have read this study and that in my opinion it conforms to acceptable standards of scholarly presentation and is fully adequate, in scope and quality, as a dissertation for the degree of Doctor of Philosophy.



---

Bhavani V. Sankar  
Assistant Professor of Aerospace  
Engineering, Mechanics and  
Engineering Science

I certify that I have read this study and that in my opinion it conforms to acceptable standards of scholarly presentation and is fully adequate, in scope and quality, as a dissertation for the degree of Doctor of Philosophy.

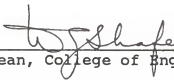


---

George Piotrowski  
Associate Professor of Mechanical  
Engineering

The dissertation was submitted to the Graduate Faculty of the College of Engineering and to the Graduate School and was accepted as partial fulfillment of the requirements for the degree of Doctor of Philosophy.

May, 1989



---

Dean, College of Engineering

---

Dean, Graduate School

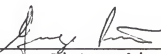
I certify that I have read this study and that in my opinion it conforms to acceptable standards of scholarly presentation and is fully adequate, in scope and quality, as a dissertation for the degree of Doctor of Philosophy.



---

Bhavani V. Sankar  
Assistant Professor of Aerospace  
Engineering, Mechanics and  
Engineering Science

I certify that I have read this study and that in my opinion it conforms to acceptable standards of scholarly presentation and is fully adequate, in scope and quality, as a dissertation for the degree of Doctor of Philosophy.

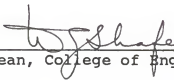


---

George Piotrowski  
Associate Professor of Mechanical  
Engineering

The dissertation was submitted to the Graduate Faculty of the College of Engineering and to the Graduate School and was accepted as partial fulfillment of the requirements for the degree of Doctor of Philosophy.

May, 1989



---

Dean, College of Engineering

---

Dean, Graduate School